NASA CR-72256

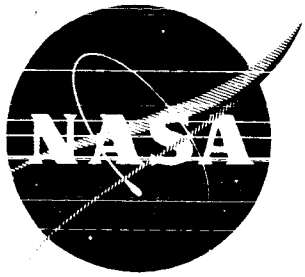

ELECTROCHEMICAL CHARACTERIZATION OF NON-AQUEOUS SYSTEMS FOR SECONDARY BATTERY APPLICATION

by

M. Shaw, O. A. Paez, R. J. Radkey, A. H. Remanick

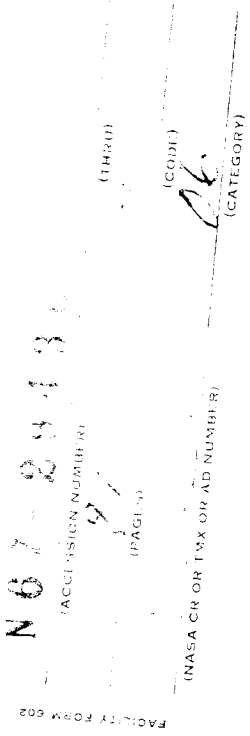

prepared for

NATIONAL AERONAUTICS AND SPACE ADMINISTRATION

CONTRACT NO. NAS 3-8509

FOURTH QUARTERLY REPORT
FEBRUARY - APRIL 1967

WHITTAKER CORPORATION
NARMCO RESEARCH & DEVELOPMENT DIVISION
3540 Aero Court
San Diego, California 92123

NASA CR-72256

ELECTROCHEMICAL CHARACTERIZATION OF NON-AQUEOUS SYSTEMS FOR SECONDARY BATTERY APPLICATION

February, 1967 - April, 1967

by

M. Shaw, O. A. Paez, R. J. Radkey, A. H. Remanick

prepared for

NATIONAL AERONAUTICS AND SPACE ADMINISTRATION

April 17, 1967

CONTRACT NAS 3-8509

Technical Management
Space Power Systems Division
National Aeronautics and Space Administration
Lewis Research Center, Cleveland, Ohio
Mr. Robert B. King

NARMCO RESEARCH AND DEVELOPMENT DIVISION
OF
WHITTAKER CORPORATION
3540 Aero Court
San Diego, California 92123

TABLE OF CONTENTS

CYCLIC VOLTAMMOGRAMS

LIST OF TABLES

ELECTROCHEMICAL CHARACTERIZATION OF NON-AQUEOUS SYSTEMS FOR SECONDARY BATTERY APPLICATION

by

M. Shaw, O. A. Paez, R. J. Radkey, A. H. Remanick

ABSTRACT

Multisweep cyclic voltammograms have been obtained for an additional two hundred systems comprising the oxides, chlorides, and fluorides of silver, copper, nickel, and cobalt in acetonitrile, butyrolactone, dimethylformamide, and propylene carbonate solutions of chlorides, perchlorates, and fluorides. Voltammograms are presented for thirty of these systems. Tabular data includes peak current density, sweep index, charge-to-discharge peak displacement, coulombic ratio, and discharge capacity. Systems exhibiting no anodic or no cathodic peaks are listed, as well as those causing instrument overload due to a combination of high current and relatively low conductance.

SUMMARY

The electrochemical characterization of nonaqueous battery systems by multi-sweep cyclic voltammetry has been continued. Cyclic voltammograms are now available on nearly six hundred systems comprising silver, copper, nickel, cobalt, zinc, cadmium, and molybdenum in chloride and fluoride solutions of acetonitrile, butyrolactone, dimethylformamide, and propylene carbonate. Solutes consist of $AlCl_3$, LiCl, $MgCl_2$, $LiClO_4$, LiF, MgF_2, $LiPF_6$, $LiBF_4$, and KPF_6. The cyclic voltammograms of thirty systems are included in this report.

During this quarter, cyclic voltammetry was initiated on AgCl, $CuCl_2$, $NiCl_2$, and $CoCl_3$ electrodes prepared by direct chlorination of the base metal. In general, nickel and cobalt chloride electrodes exhibit low or negligible electrochemical activity in agreement with earlier data on nickel and cobalt metal. When activity was indicated, it was usually only anodic, with no cathodic current evident, which may have been due to immediate dissolution of the anodic product. Measurements were continued on AgF_2, CuF_2, NiF_2, and CoF_3 electrodes prepared by direct fluorination of the base metal.

Cyclic voltammograms were not recordable in BF_3 and PF_5 solutions due to voltage overload of the instrumentation caused by a combination of appreciably high current and relatively low conductance (10^{-4} ohm^{-1} cm^{-1}) for these solutions.

Tables are presented listing system parameters derived from the cyclic voltammograms. These tables include data on peak current densities, sweep index, anodic to cathodic peak displacement, coulombic ratio, and discharge capacity. Listed also are those systems exhibiting no anodic or cathodic peaks, as well as those systems causing instrument overload.

INTRODUCTION

The purpose of this program is to conduct a molecular level screening by the cyclic voltammetric method on a large number of electrochemical systems in nonaqueous electrolytes, and to characterize them as to their suitability for use in high energy density secondary batteries.

Since the release and storage of energy in a battery is initiated at the molecular level of the reaction, and therefore dependent on the charge and mass transfer processes, it is essential that screening be conducted at this level, in order to eliminate those systems whose electrode processes are inadequate for secondary battery operation.

I. RESULTS

A. ANALYSIS OF CYCLIC VOLTAMMOGRAMS

Table I lists the conductivities of the solutions screened during this quarter. Tables II and III list the electrochemical systems screened during the fourth quarter of this program. This represents a total of 200 systems. Curve analysis was accomplished by dividing all systems into two major groups:

1. Systems involving chloride and perchlorate electrolytes
2. Systems involving fluoride electrolytes

Each main group was then subdivided according to the identity of the working electrode. Each of these subgroups was further broken down according to the identity of the solvent portion of the solution. The cyclic voltammograms are then discussed in terms of the total solution. This classification facilitates data analysis, and has permitted a more significant correlation among the electrochemical systems.

Except in those cases where the metal is converted to a cathodic material prior to assembly in the measuring cell, the working electrode is the base metal itself. During the voltage sweep, the metal is oxidized to some species, this anodic product then serving as the cathode which is subsequently reduced during the cathodic portion of the sweep. Each sweep cycle thus corresponds to a charge-discharge cycle. In the absence of complicating factors, it is assumed that chloride cathodes would be formed in chloride electrolytes, and fluoride cathodes in fluoride electrolytes.

Each cyclic voltammogram is identified by a CV number and labelled according to the electrochemical system , sweep rate, temperature, and zero reference, representing the open circuit voltage (ocv) of the working electrode with respect to the indicated reference electrode. The current axis is in units of ma/cm^2, each unit being of variable scale depending on the X-Y

recorder sensitivity setting. A maximum sensitivity of 0. 1 ma/cm^2/cm division has been established to avoid exaggerating the current background of poor systems. The sweep is always in a clockwise direction, the potential becoming more positive to the right. Positive currents represent anodic (charge) reactions, and negative currents represent cathodic (discharge) reactions. The voltage axis units are relative to the ocv so that voltage units are in terms of electrode polarization.

For comparative purposes, current density magnitude is classified according to very high (more than 300 ma/cm^2), high (100-300 ma/cm^2), medium high (50-100 ma/cm^2), medium low (10-50 ma/cm^2), low (1-10 ma/cm^2), and very low (less than 1 ma/cm^2).

Analysis is based on the cyclic voltammograms obtained at the lowest sweep rate, 40 mv/sec, except where additional information is required from the higher sweep rate curves to aid in the analysis.

TABLE I

ELECTROLYTE CONDUCTIVITY*

Electrolyte	Molality m	Conductivity $ohm^{-1}\ cm^{-1}$
Acetonitrile-$AlCl_3$	1.00	3.7×10^{-2}
Acetonitrile-$LiClO_4$	0.75	3.0×10^{-2}
Dimethylformamide-LiCl+$LiClO_4$	0.75	1.9×10^{-2}
Dimethylformamide-$LiClO_4$	0.50	1.8×10^{-2}
Acetonitrile-$LiPF_6$	0.50	1.7×10^{-2}
Acetonitrile-$LiBF_4$	0.50	1.6×10^{-2}
Acetonitrile-LiCl+$AlCl_3$	0.25 (a)	1.5×10^{-2}
Butyrolactone-$LiClO_4$	0.75	1.1×10^{-2}
Butyrolactone-LiCl+$AlCl_3$	0.50	1.1×10^{-2}
Butyrolactone-$AlCl_3$	0.50	1.0×10^{-2}
Dimethylformamide-LiCl+$AlCl_3$	0.50 (b)	1.0×10^{-2}
Dimethylformamide-LiCl+$MgCl_2$	0.50 (s)	9.0×10^{-3}
Propylene carbonate-LiCl+$AlCl_3$	0.50 (c)	8.9×10^{-3}
Dimethylformamide-LiCl	0.75	8.7×10^{-3}
Dimethylformamide-$MgCl_2$	0.50 (s)	8.4×10^{-3}
Butyrolactone-LiCl+$LiClO_4$	0.50	8.3×10^{-3}
Propylene carbonate-$AlCl_3$	0.50	8.0×10^{-3}
Propylene carbonate-$LiClO_4$	1.00	6.2×10^{-3}
Propylene carbonate-$LiPF_6$	0.25	5.9×10^{-3}
Propylene carbonate-LiCl+$MgCl_2$	< 0.50 (s)	5.8×10^{-3}

* In order of decreasing conductivity

(a) Initially 0.25 m in $AlCl_3$, saturated at less than 0.25 m with LiCl.

(b) Initially 0.5 m in LiCl, saturated at less than 0.5 m with $AlCl_3$.

(c) Initially 0.5 m in $AlCl_3$, saturated at less than 0.5 with LiCl.

(s) Saturated.

TABLE I (Cont'd.)

Electrolyte	Molality m	Conductivity $ohm^{-1}\ cm^{-1}$
Dimethylformamide-$LiBF_4$	0.50	5.7×10^{-3}
Dimethylformamide-$AlCl_3$	0.50 (s)	5.4×10^{-3}
Butyrolactone-$LiCl+MgCl_2$	0.75 (s)	5.4×10^{-3}
Propylene carbonate-$LiBF_4$	0.50	4.2×10^{-3}
Dimethylformamide-BF_3	0.50	3.2×10^{-3}
Dimethylformamide-$Mg(BF_4)_2$	0.25	2.8×10^{-3}
Dimethylformamide-$LiPF_6$	0.50	2.7×10^{-3}
Propylene carbonate-$MgCl_2$	0.50	2.4×10^{-3}
Acetonitrile-PF_5	0.50	2.2×10^{-3}
Butyrolactone-$MgCl_2$	0.50 (s)	1.3×10^{-3}
Acetonitrile-$Mg(BF_4)_2$	0.50 (s)	9.2×10^{-4}
Propylene carbonate-PF_5	0.06	7.9×10^{-4}
Acetonitrile-LiCl	0.50	7.1×10^{-4}
Acetonitrile-$MgCl_2$	0.50	6.3×10^{-4}
Butyrolactone-BF_3	0.50	6.2×10^{-4}
Dimethylformamide-PF_5	0.50	3.9×10^{-4}
Propylene carbonate-$Mg(BF_4)_2$	0.25	2.2×10^{-4}
Propylene carbonate-BF_3	0.50	1.5×10^{-4}
Acetonitrile-BF_3	0.50	7.4×10^{-5}

(s) Saturated

TABLE II ELECTROCHEMICAL SYSTEMS SCREENED - CHLORIDE (or PERCHLORATE) ELECTROLYTES

Solute \ Solvent	Acetonitrile	Butyrolactone	Dimethylformamide	Propylene carbonate
LiCl		$AgCl$, $CuCl_2$ $NiCl_2$, $CoCl_3$	$AgCl$, $CuCl_2$, $NiCl_2$ $CoCl_3$	
$AlCl_3$	$AgCl$, $CuCl_2$, $NiCl_2$ Co, CoO, $CoCl_3$	$AgCl$, $CuCl_2$ $NiCl_2$, Co, $CoCl_3$	$AgCl$, $CuCl_2$, $NiCl_2$ Co, CoO, $CoCl_3$	$AgCl$, $CuCl_2$, NiO $NiCl_2$, Co, CoO $CoCl_3$
$LiCl + AlCl_3$	$AgCl$, AgF_2, $CuCl_2$ CuF_2, $NiCl_2$, NiF_2, Co CoO, $CoCl_3$, CoF_3	$AgCl$, AgF_2, $CuCl_2$ CuF_2, $NiCl_2$, NiF_2 Co, CoO, $CoCl_3$ CoF_3	$AgCl$, $CuCl_2$, $NiCl_2$ CoO, $CoCl_3$	$AgCl$, AgF_2, $CuCl_2$ CuF_2, $NiCl_2$, NiF_2 Co, CoO, $CoCl_3$, CoF_3
$LiClO_4$	$AgCl$, $CuCl_2$, $NiCl_2$ $CoCl_3$	$AgCl$, $CuCl_2$ $NiCl_2$, $CoCl_3$	$AgCl$, $CuCl_2$, $NiCl_2$ $CoCl_3$	$AgCl$, $CuCl_2$, $NiCl_2$ $CoCl_3$
$LiCl + LiClO_4$		$AgCl$, $CuCl_2$ $NiCl_2$, $CoCl_3$	$AgCl$, $CuCl_2$, $NiCl_2$ $CoCl_3$	
$MgCl_2$	$AgCl$, $CuCl_2$, $NiCl_2$, Co CoO, $CoCl_3$, CoF_3	$AgCl$, $CuCl_2$, $NiCl_2$ Co, CoO, $CoCl_3$	$AgCl$, $CuCl_2$, $NiCl_2$, Co CoO, $CoCl_3$, CoF_3	$AgCl$, $CuCl_2$, NiO $NiCl_3$, Co, CoO $CoCl_3$, CoF_3
$LiCl + MgCl_2$		$AgCl$, $CuCl_2$, $NiCl_2$ CoO, $CoCl_3$	$AgCl$, $CuCl_2$, Co, $CoCl_3$	$AgCl$, $CuCl_2$, $NiCl_2$ Co , $CoCl_3$

TABLE III ELECTROCHEMICAL SYSTEMS SCREENED - FLUORIDE ELECTROLYTES

Solvent / Solute	Acetonitrile	Butyrolactone	Dimethylformamide	Propylene carbonate
$LiBF_4$	Ag, Cu, Ni, Co		Ag, Cu, Ni, Co	Ag, Cu, Ni
$LiPF_6$	AgCl, $CuCl_2$, $NiCl_2$ $CoCl_3$		AgCl, $CuCl_2$, $NiCl_2$ $CoCl_3$	AgCl, $CuCl_2$, $NiCl_2$ $CoCl_3$
$Mg(BF_4)_2$	AgF_2, CuF_2, NiF_2, CoF_3		AgF_2 CuF_2, NiF_2 CoF_3	Ag, AgF_2, Cu, CuF_2 Ni, NiF_2, Co, CoF_3
BF_3	AgF_2, CuF_2, NiF_2 CoF_3	AgF_2, CuF_2, NiF_2, CoF_3	AgF_2, CuF_2, NiF_2 CoF_3	AgF_2, CuF_2, NiF_2 CoF_3
PF_5	AgF_2, CuF_2, NiF_2 CoF_3		AgF_2, CuF_2, NiF_2 CoF_3	AgF_2, CuF_2, NiF_2 CoF_3

1. Systems Involving Chloride and Perchlorate Electrolytes

a. Silver Chloride Electrode

(1) Acetonitrile solutions

Silver chloride in acetonitrile-$AlCl_3$ shows voltage overload on the cathodic sweep, whereas essentially no anodic current is evident. This indicates discharge of available material with no subsequent reformation on charge. This is in contrast to the reaction of silver which exhibits anodic reaction (Ref. 1). Using $MgCl_2$ as the solute, the reaction of silver chloride exhibits a complex reaction type accompanied by low currents. The overall reaction type and peak currents are of the same order as that of silver in this electrolyte (Ref. 2, p. 28).

The cyclic voltammogram for AgCl in LiCl+$AlCl_3$ solution is shown in Figure 1 (CV-1969). High, sharp peaks are obtained for both the charge and discharge reactions. Although the peak current densities are in the very high range (>700 ma/cm^2), they are not as high as obtained with silver electrode in the same solution, which results in voltage overload (Ref. 1). In the case of $LiClO_4$ solution, AgCl exhibits excellent sweep curves during the pre-recording cycling, with high current densities (1 amp/cm^2), but current overload in the cathodic direction occurs during the tenth cycle.

(2) Butyrolactone solutions

The cyclic voltammogram for AgCl in butyrolactone-$AlCl_3$ shows two well-defined peaks (Figure 2, CV-2209). Current densities for both the anodic and cathodic reactions are relatively high. However, since the peak-to-peak voltage separation is large, this system would probably not make an efficient secondary. These results are similar to those previously obtained using Ag in this electrolyte. The proportionately larger cathodic area is probably due to discharge of original AgCl. AgCl in LiCl solution produces

current overload as contrasted with silver metal in the same solution which gave low currents (Ref. 1, p. 35). These low currents, and the failure to reach an anodic peak, were attributed to the low availability of chloride ions, as indicated by low solution conductivity. The existence of very high currents for AgCl may result from high chloride concentration existing at the reaction interface. AgCl in $LiCl+AlCl_3$ solution shows a double anodic peak and a broad cathodic peak, both in the high current density range (Figure 3, CV-1887). Blue discoloration of the solution was observed. A similar type of double anodic peak was observed for silver metal in dimethylformamide-$MgCl_2$ (Ref. 1, p. 48).

Voltage overload is exhibited in $MgCl_2$ solution, which may possibly be due to electrode resistance since a combination of solution resistance and current should not have resulted in overload. Silver metal in the same solution (Ref. 1, p. 36) gives a comparable anodic current value, but the cathodic current is three-fold smaller. A mixture of LiCl and $MgCl_2$ results in the voltammogram shown in Figure 4 (CV-2251) for the AgCl electrode. Neither current nor voltage overload occurs as for the individual salts, but instead the curve resembles that of silver metal in the same electrolyte (Ref. 1, p. 37). Current overload in both the anodic and cathodic directions results in $LiClO_4$ solution after initial recording of sharp, very high c. d. peaks, accompanied by dark brown discoloration of the solution. LiCl-$LiClO_4$ solution also produces current overload. This is in contrast to silver metal which registered anodic and cathodic peaks in the order of 128 ma/cm^2 (Ref. 1, p. 39).

(3) Dimethylformamide solutions

AgCl in LiCl solution gives very high current densities (1. 5 $amps/cm^2$) and a dark brown discoloration of the solution. The peak-to-peak displacement is less than 100 mv. The sweep curve obtained in $LiCl+AlCl_3$ solution

(Figure 5, CV-1914) is peculiar in that the cathodic peak occurs at a more positive potential than the anodic peak, which raises the possibility that the anodic peak does not represent formation of AgCl. The peak representing reduction of AgCl is sharp and well formed. AgCl in $AlCl_3$ solution results in voltage overload and brown discoloration, whereas AgCl in $LiClO_4$ solution produces current overload with a black discoloration. The cyclic voltammogram in $MgCl_2$ solution (Figure 6, CV-2131) shows a high ΔV_p value. The reduction of AgCl in $LiCl+MgCl_2$ solution shows a sharp peak (Figure 7, CV-2281), but the anodic reaction, if it represents oxidation of Ag to AgCl, is poor. At least two distinct anodic reactions are indicated. A similar complex anodic curve was obtained for Ag in the same solution (Ref. 1, p. 47), but a small second reduction peak was also present. Substitution of $LiClO_4$ for $MgCl_2$ results in two well-defined anodic peaks, and the beginning of a third reaction at a highly positive potential, as shown in Figure 8 (CV-2231). The cathodic reaction is more complex, however, and the primary cathodic reaction is not as efficient as for $LiCl+MgCl_2$. The presence of LiCl prevented current overload as occurred for AgCl in dimethylformamide-$LiClO_4$ solution, even though the solution conductivities are nearly identical.

(4) Propylene carbonate solutions

AgCl in $LiCl+AlCl_3$ solution exhibits only low currents with no peak formation, contrasting with high current peaks for silver metal in the same solution (Ref. 3, p. 59). $AlCl_3$ alone results in very high currents. During the pre-recording cycles, the cathodic current density was many times higher than the anodic. A large ΔV_p exists, comparing with the results obtained for Ag metal (Ref. 3, p. 74), except that the currents are an order of magnitude larger in the case of AgCl. Current overload is obtained in $LiClO_4$ solution, which was not the case for silver in the corresponding solution (Ref. 1, p. 56). The sweep curve in $MgCl_2$ solution (Figure 9,

CV-2069) is comparable to that obtained for silver in the same solution (Ref. 1, p. 54) except that sharper peaks are obtained, due probably to measurement of Ag in the older cell. AgCl in $LiCl+MgCl_2$ solution results in much lower current densities than for Ag in the same solution (Ref. 1, p. 55).

b. Silver Difluoride Electrode

AgF_2 shows medium low to very low currents in $LiCl+AlCl_3$ solutions of acetonitrile, butyrolactone, and propylene carbonate, although peaks are observed in all cases, the cathodic peaks being sharper than the anodic peaks.

As stated in an earlier report (Ref. 2), the low currents may result from a relatively high electrode resistance due to the formed AgF_2 layer on the electrode.

c. Copper Chloride Electrode

(1) Acetonitrile solutions

Copper chloride in acetonitrile-$AlCl_3$ exhibits current overload in both the anodic and cathodic regions indicating high current densities for undefined reactions. However, since the reaction of Cu in this electrolyte is accompanied by the formation of a soluble product (Ref. 1, p. 23), it is not expected that the present system is of value. Very high anodic and cathodic peaks (400 - 450 ma/cm^2) are obtained in $LiCl+AlCl_3$ solution with visible dissolution of the $CuCl_2$, in agreement with earlier data on copper metal in the corresponding solution (Ref. 1). The 40 mv/sec sweep curve for $CuCl_2$ in $LiClO_4$ is of poor reproducibility, but curves obtained at 200 mv/sec indicate two separate reduction reactions not observed for copper metal (Ref. 3, p. 38). Use of $MgCl_2$ in acetonitrile results in voltage overload. In this instance, there is no evidence of cathodic current. This is similar to the results for Cu electrode.

(2) Butyrolactone solutions

The cyclic voltammogram of copper chloride in butyrolactone-$AlCl_3$ exhibits reasonably sharp anodic and cathodic peaks although multiple reactions are apparently involved in both reactions (Fig. 10, CV-2208). The anodic reaction is similar to that for Cu in this electrolyte (Ref. 1, p. 57) except for the magnitude of the peak current density. In the latter case, the anodically-formed copper chloride dissolved in the electrolyte so that the cathodic peak decreased with decreasing sweep rate relative to the anodic peak. In the present case, sufficient chemically-formed $CuCl_2$ is present to give an extremely high discharge current.

The voltammogram for $CuCl_2$ in $LiCl+MgCl_2$ is shown in Figure 11 (CV-2256). A single pronounced charge and discharge peak occurs which are probably not related to the same reaction. Current densities are considerably lower than for the $AlCl_3$ case, possibly due to a lower chloride ion availability. Dissolution of positive material is evident.

The anodic portion of the sweep curve at 40 mv/sec is extremely erratic in LiCl solution, with voltage overload occurring at the higher sweep rates. The curve obtained for $CuCl_2$ in $LiCl+AlCl_3$ solution (Figure 12, CV-1902) is nearly identical to that for copper in $LiClO_4+AlCl_3$ (Ref. 1, p. 58). A very high anodic peak (800 ma/cm^2) and very high cathodic peak (960 ma/cm^2) are obtained in $LiClO_4$ solution. Considerable concentration polarization is indicated. Non-reproducible oscillations occur at highly positive potentials. Current overload results at the higher sweep rates. In $LiCl+LiClO_4$ solution, two anodic peaks and a single cathodic peak are exhibited, all at high current densities. The peaks are broad, indicating extensive polarization.

The cyclic voltammograms for $CuCl_2$ in butyrolactone-$MgCl_2$ obtained at 200, 80, and 40 mv/sec are shown in Figure 13 (CV's-2102, 2104, and 2105).

The cathodic peak moves to more anodic potentials with decreasing sweep rate, so that at 40 mv/sec it is slightly more positive than the first anodic peak. This would indicate that the charge reaction occurs at a lower voltage than the discharge if the first anodic peak represents the reverse process of the discharge reaction. On the other hand, the second anodic peak may represent the charge reaction corresponding to the cathodic peak resulting in a larger ΔV_p value, and indicating poorer rechargeability for the system. (These results indicate the difficulty in interpreting cyclic voltammograms of preformed electrodes recorded after a minimum of 10 charge-discharge cycles.) The higher value for the anodic peaks at the lower sweep rates is an exception to the general observation that peak height decreases with decreasing sweep rate, as shown by the relative heights of the cathodic peaks.

(3) Dimethylformamide solutions

Copper chloride in $MgCl_2$+LiCl solution exhibits a rather complex charge reaction, as shown in Figure 14 (CV-2286). An excellent discharge, however, is indicated, having a very high peak current density and negligible polarization. The initial anodic peak is absent at 200 mv/sec, and the higher oxidation peaks are poorly reproducible at all sweep rates. Substitution of $LiClO_4$ for $MgCl_2$ improves the anodic characteristics of the system although multiple peaks are still observed which are reproducible. The sweep curve for this system is shown in Figure 15 (CV-2236). There is a decrease in the peak current density for the cathodic reaction (compared to $MgCl_2$+LiCl) as well as an increase in polarization for this system. The reaction type is similar to that observed for copper in the same electrolyte (Ref. 1, p. 61), although the peak current densities are lower for the copper chloride electrode.

The 40 mv/sec voltammogram for $CuCl_2$ in LiCl solution indicates no appreciable anodic or cathodic reaction; however, during the pre-recording cycling at the 200 mv/sec sweep rate, current overload occurs during the anodic sweep, and a maximum current density of 400 ma/cm^2 is obtained during the cathodic sweep. The pre-recording currents may represent reactions involving copper chloride which dissolved prior to recording. The solubility of anodically-formed $CuCl_2$ was reported earlier (Ref. 1, p. 59). If unreacted copper metal was exposed, however, it is not clear why a sweep curve typical of copper in this solution was not obtained.

Non-reproducible anodic curves are obtained at all sweep rates for $CuCl_2$ in $AlCl_3$ and $LiCl+AlCl_3$ solutions. A single cathodic peak results in the latter system having a very high current density (960 ma/cm^2). No anodic or cathodic reaction is evident in $LiClO_4$ solution. Multiple cathodic peaks are obtained in $MgCl_2$ solution, as well as a single sharp cathodic peak of medium low current density.

(4) Propylene carbonate solutions

$CuCl_2$ in $LiCl+AlCl_3$ solution exhibits current overload during the cathodic sweep, and a maximum current of 2 $amps/cm^2$ during the anodic sweep. The sweep curve for $AlCl_3$ solution is shown in Figure 16 (CV-2147), and for $LiClO_4$ solution in Figure 17 (CV-1999). The latter system has been under investigation as a primary using a lithium negative. The cyclic voltammogram for $CuCl_2$ in $MgCl_2$ solution is given in Figure 18 (CV-2064). A soluble anodic product is indicated according to an increasing anode-to-cathode peak ratio with decreasing sweep rate. This confirms earlier data obtained with copper metal in the corresponding electrolyte. Figure 19 (CV-2433) shows the cyclic voltammogram for $CuCl_2$ in $LiCl+MgCl_2$ solution, confirming that $CuCl_2$ is soluble in this electrolyte. Cu in the same electrolyte formed a solid state soluble anodic product (Ref. 1, p. 68).

d. Copper Fluoride Electrode

(1) Acetonitrile solutions

Similar to $CuCl_2$ and Cu in $LiCl+AlCl_3$ solution, the cyclic voltammograms for CuF_2 indicate dissolution of the cathode material. $CuCl_2$ exhibits voltage overload at the higher sweep rates, whereas high current peaks are obtainable at these sweep rates with CuF_2.

(2) Butyrolactone solutions

Figure 20 (CV-1882) shows the cyclic voltammogram for CuF_2 in $LiCl+AlCl_3$ solution, obtained at 40 mv/sec compared with curves obtained at 200 and 80 mv/sec, (Figure 21, CV-1879, and Figure 22, CV-1881 respectively). This represents a typical example of cathode dissolution resulting in a relative decrease of cathodic peak height with decreasing sweep rate, and which may disappear entirely at the lowest sweep rate, as occurs in this case. The cyclic voltammogram obtained at the highest sweep rate (Figure 21) represents the curve for an excellent system (including an extremely high discharge current), the cathode of which unfortunately is soluble. The cathodic peak is greatly decreased at 80 mv/sec (Figure 22) due to less material being available for reduction at the electrode because of cathode dissolution (reduction of a solid state material). A second reduction reaction exists at a much more negative potential. The peak representing this reaction is more pronounced at 40 mv/sec, while the primary reduction reaction is now entirely absent (Figure 20). No color change could be detected during the measurements since the solution was dark yellow-brown prior to its use.

(3) Propylene carbonate solutions

CuF_2 in $LiCl+AlCl_3$ solution exhibits an extremely high, sharp cathodic peak (1.6 amp/cm^2), but poorly formed, medium high anodic peaks, the sweep curve resembling that of CuO in propylene carbonate-$LiClO_4$ (Ref. 1, p. 69).

This system would not be recommended for secondary battery application, although it might be applicable in a high rate, primary battery.

e. Nickel Oxide Electrode

NiO shows a medium low anodic peak, with virtually no discharge reaction, in propylene carbonate-$AlCl_3$, whereas no anodic or cathodic reaction is observed in propylene carbonate-$MgCl_2$.

f. Nickel Chloride Electrode

$NiCl_2$ fails to exhibit discharge peaks in all systems except butyrolactone-LiCl and dimethylformamide-LiCl+$LiClO_4$. In those instances where cathodic activity was indicated, the maximum current density was usually less than 0.5 ma/cm^2. These results are comparable to those previously found for nickel systems.

(1) Acetonitrile solutions

Anodic current overload is obtained for $NiCl_2$ in $AlCl_3$ solutions with or without LiCl, but only a low anodic current at +1.0 v in $LiClO_4$ solution.

(2) Butyrolactone solutions

A medium high anodic peak and medium low cathodic peak (separated by 1.0 v) are obtained for $NiCl_2$ in LiCl solution. Very low anodic currents are produced in LiCl+$AlCl_3$ and $MgCl_2$ solutions. A low anodic peak is shown in $LiClO_4$ solution. LiCl+$LiClO_4$ solution shows low anodic and cathodic activity occurring at the extremes of the voltage range scanned, with current densities less than 6 ma/cm^2.

(3) Dimethylformamide solutions

$NiCl_2$ shows negligible anodic current in $MgCl_2$, LiCl, and $LiClO_4$ solutions. Voltage overload is obtained in $AlCl_3$, and current overload in $LiCl+AlCl_3$ solution, in each case the solution becoming dark green in color. A reasonably well-defined anodic peak is exhibited by dimethylformamide-$LiCl+LiClO_4$, accompanied by a broad cathodic peak having a peak current density of 45 ma/cm^2, but displaced by 1.2 v. Voltage overload occurs in $LiCl+MgCl_2$ solution.

(4) Propylene carbonate solutions

$NiCl_2$ shows no appreciable current in $MgCl_2$, $AlCl_3$, and $LiClO_4$ solutions, and only a low anodic peak in $LiCl+AlCl_3$ solution. The cyclic voltammogram for nickel chloride in $LiCl+MgCl_2$ solution is shown in Figure 23 (CV-2438). Although anodic peaks of about 100 ma/cm^2 are obtained, no discharge reaction is evident, typical of many of the $NiCl_2$ systems. In contrast, nickel metal yields anodic currents less than 0.1 ma/cm^2, suggesting that chlorination results in activation of the nickel surface allowing irreversible anodic reaction.

g. Nickel Fluoride Electrode

Nickel fluoride exhibits no cathodic current in the chloride systems studied. Whereas anodic current is virtually absent in propylene carbonate-$LiCl+AlCl_3$, current overload results in acetonitrile-$LiCl+AlCl_3$ solution accompanied by a milky-white discoloration in solution with considerable gassing. A medium low anodic peak occurs at +1.0 v in butyrolactone-$LiCl+AlCl_3$ solution.

h. Cobalt Electrode

No cathodic activity is indicated for all cobalt systems screened.

(1) Acetonitrile solutions

Cobalt exhibits anodic voltage overload (c. d. is 80 ma/cm^2) in acetonitrile-$MgCl_2$, with virtually zero discharge current. Although the anodic current density is nearly twice as high for acetonitrile-$AlCl_3$, voltage overload is absent, which is explained by the higher solution conductivity for the latter electrolyte. Again, no cathodic reaction is evident. Anodic current overload occurs in LiCl-$AlCl_3$ solution.

(2) Butyrolactone solutions

Cobalt in butyrolactone-$AlCl_3$ exhibits two distinct anodic peaks and zero discharge current. The anodic peaks are in the same height ratio as for Co in propylene carbonate-$AlCl_3$ (Figure 24, CV-2173), but the current densities are twice as high. LiCl+$AlCl_3$ shows a high anodic current density peak, but no discharge current. Anodic voltage overload results in the case of butyrolactone-$MgCl_2$.

(3) Dimethylformamide solutions

No anodic or cathodic reaction is observed in dimethylformamide-$MgCl_2$ solution with or without LiCl. $AlCl_3$ solution shows anodic voltage overload and zero cathodic reaction.

(4) Propylene carbonate solutions

The cyclic voltammogram for cobalt in propylene carbonate-$AlCl_3$ is shown in Figure 24 (CV-2173). Although having no value for battery application since no discharge reaction is evident, the curve is of interest because of the existence of three distinct anodic peaks corresponding to the theoretically available number of electrons per mole. This, however, may be simply fortuitous.

The sweep curve in propylene carbonate-$MgCl_2$ exhibits a medium high, sharp anodic peak and virtually no discharge current. In propylene carbonate-$LiCl+AlCl_3$, two distinctly separated anodic peaks occur, each in the medium low range, accompanied by a medium low cathodic current density at -1.0 v. Cobalt exhibits a single high anodic peak (90 ma/cm^2) in $LiCl+MgCl_2$ solution, but again no discharge reaction is evident.

i. Cobalt Oxide Electrode

The results obtained for CoO nearly coincide with those obtained for cobalt in the corresponding solutions. Thus, anodic current overload occurs in acetonitrile-$LiCl+AlCl_3$, and anodic voltage overload in butyrolactone-$MgCl_2$ and dimethylformamide-$AlCl_3$. Again, zero discharge current exists for all systems screened. A broad anodic peak of low range is exhibited by butyrolactone-$LiCl+AlCl_3$. In contrast to cobalt, however, which gives very low currents in dimethylformamide-$MgCl_2$, CoO has a very high anodic peak at +0.8 v. A medium low anodic current maximum is shown for $LiCl+AlCl_3$ in the same solvent. Negligible anodic current is obtained in propylene carbonate-$LiCl+AlCl_3$, and only low current for $MgCl_2$ in the same solvent.

j. Cobalt Chloride Electrode

As is the case for cobalt and cobalt oxide, none of the cobalt chloride systems show desirable cyclic voltammograms. In nearly all cases no discharge reaction is indicated.

(1) Acetonitrile solutions

Similar to Co and CoO, cobalt chloride in $LiCl+AlCl_3$ gives anodic current overload, again showing blue discoloration of the solution. $LiClO_4$ solution shows a very high anodic peak at +1.0 v; a medium low cathodic peak is displaced 1.46 volts negative to the anodic peak.

(2) Butyrolactone solutions

Again like Co and CoO, cobalt chloride shows anodic voltage overload in $MgCl_2$ solution. A sharp anodic peak in the high current density range is exhibited in $LiCl+AlCl_3$ solution, identical in shape and magnitude to that obtained for Co in the same solution (Figure 25, CV-1872). A very high density peak is obtained in LiCl solution, with current overload at the higher sweep rates. Dissolution of cobalt chloride was observed, so that cobalt metal was probably exposed accounting for the very high anodic currents (Co in butyrolactone-LiCl gives voltage overload, Ref. 2). The cyclic voltammogram for cobalt chloride in $LiClO_4$ is identical to that obtained for Co in the same solution (Ref. 2, p. 42). Unlike most cobalt systems which exhibit exceedingly large peak-to-peak separation (usually 1.5 - 1.7 v), $CoCl_3$ in butyrolactone-$LiCl+MgCl_2$ (Figure 26, CV-2266) shows a ΔV_p of about 0.6 v, even though the amount of cathodic activity itself is negligible. In general, results are comparable to those obtained with Co electrode.

(3) Dimethylformamide solutions

Anodic voltage overload is obtained in $AlCl_3$ solution, as was the case for Co in the same solution. Current overload results in the case of $LiCl+AlCl_3$, corresponding to voltage overload obtained for Co in the same system (Ref. 2). Very low currents with no peak formation are exhibited in LiCl solution. This is in sharp contrast to Co in the same solution which exhibits anodic current overload (Ref. 2). However, $CoCl_3$ in $MgCl_2$ exhibits negligible currents as was the case for Co in the same solution. Again $CoCl_3$ behaves like cobalt metal in $LiClO_4$ solution (Ref. 2) in that negligible currents are obtained.

(4) Propylene carbonate solutions

The sweep curves for cobalt chloride in $LiClO_4$ solution, as well as in $MgCl_2$, $AlCl_3$, and $LiCl+AlCl_3$ solutions, are identical to those obtained for cobalt metal in the corresponding solutions.

The results obtained for cobalt chloride can in all cases be explained by dissolution of the pre-formed cobalt chloride in the solutions tested. A discrepancy exists in the case of dimethylformamide-LiCl (in which dissolution giving a blue discoloration was also observed).

2. Systems Involving Fluoride Electrolytes

a. Silver Electrode

Silver electrodes give either current or voltage overload in the solutions screened. Anodic current overload is obtained for $LiBF_4$ solutions of acetonitrile and dimethylformamide. No discharge is evident in the acetonitrile solution. The cathodic current was not recorded for the dimethylformamide solution. Propylene carbonate solutions of $LiBF_4$ and $Mg(BF_4)_2$ give voltage overload. A maximum anodic current density of 3.2 amps/cm^2 was measured for the $LiBF_4$ solution, compared with 400 ma/cm^2 for the discharge current. 200 ma/cm^2 were obtained in the $Mg(BF_4)_2$ solution for both the charge and discharge currents. The $LiBF_4$ data represent repeats of earlier measurements (Ref. 3, p. 39, and Ref. 1, p. 71) obtained with solutions prepared from commercial $LiBF_4$. The present data was obtained with solutions of $LiBF_4$ prepared in-situ (Ref. 2, p. 84).

b. Silver Chloride Electrode

Silver chloride in acetonitrile-$LiPF_6$ shows very high and erratic anodic currents (approximately 1 amp/cm^2), but relatively low cathodic peaks. Cathodic current overload is obtained for AgCl in dimethylformamide-$LiPF_6$. A maximum anodic current density of 400 ma/cm^2 is indicated. Propylene carbonate-$LiPF_6$ (Figure 27, CV-2499), shows broad, highly polarized, anodic and cathodic peaks with current densities of about 100 ma/cm^2. The cathodic area is slightly larger than the anodic area, suggesting discharge of the original AgCl, in addition to discharge of products formed during the anodic reaction.

c. Silver Difluoride Electrode

Voltage overload is obtained for AgF_2 in BF_3 and PF_5 solutions of all solvents. This compares with the results obtained for silver metal (Ref. 2, p. 69). High to extremely high current densities are evident for both the charge and discharge reactions. Similar results are obtained for $Mg(BF_4)_2$ solutions, except that no discharge current is evident in acetonitrile.

d. Copper Electrode

The cyclic voltammogram for Cu in acetonitrile-$LiBF_4$ is shown in Figure 28 (CV-2362). Relatively sharp peaks and a low peak-to-peak separation (100 mv) show low polarization. The low discharge-to-charge coulombic ratio (23%) may possibly result from partial dissolution of the anodic products of the electrochemical reaction, although the sweep rate behavior is consistent with that expected for an insoluble cathodic reactant. Copper in dimethylformamide-$LiBF_4$ shows very high anodic but zero cathodic currents. Propylene carbonate-$LiBF_4$ shows very high anodic and cathodic currents causing voltage overload. $Mg(BF_4)_2$ solution of propylene carbonate also exhibits voltage overload with copper, but with a much lower cathodic current, 80 ma/cm^2 compared with 4 amps/cm^2 for the $LiBF_4$ solution.

e. Copper Chloride Electrode

The cyclic voltammogram of copper chloride in dimethylformamide-$LiPF_6$ is shown in Figure 29 (CV-2300). Very high charge and discharge currents are obtained. An excellent discharge reaction is indicated - negligible polarization and excellent voltage regulation. A ΔV_p value of only 60 mv is observed. The anodic curve indicates a satisfactory charge reaction, as long as the charge potential in a practical system is maintained within 0.1 - 0.2 v positive to the open circuit value. Further oxidation occurs on the return anodic sweep, as indicated by the repeated peak.

The cyclic voltammogram of $CuCl_2$ in acetonitrile-$LiPF_6$ is shown in Figure 30 (CV-2454) and is comparable to copper metal in the same solution (Ref. 2, p. 45) except that the peak-to-peak separation is slightly larger (110 mv compared with 90 mv for Cu). $CuCl_2$ in propylene carbonate-$LiPF_6$ (Figure 31, CV-2504) shows a broad anodic and cathodic peak of medium low current density. Two anodic peaks are observed at 200 mv/sec.

f. Copper Fluoride Electrode

Similar to AgF_2, copper fluoride electrodes exhibit voltage overload in all BF_3 solutions. Unlike AgF_2, however, the discharge current is negligible for dimethylformamide and propylene carbonate. These electrodes also exhibit voltage overload in acetonitrile, dimethylformamide, and propylene carbonate solutions of both PF_5 and $Mg(BF_4)_2$ solutions. Exceedingly high discharge currents in excess of 1 amp/cm^2 are exhibited by acetonitrile and dimethylformamide solutions of PF_5, and dimethylformamide-$Mg(BF_4)_2$.

g. Nickel Electrode

Repeat measurements have been made in $LiBF_4$ solution. Nickel in acetonitrile-$LiBF_4$ shows a very high anodic current but no cathodic discharge. Nickel dimethylformamide-$LiBF_4$ is similar and shows a low, broad anodic peak but no discharge current. In propylene carbonate-$LiBF_4$ solution, nickel shows very low anodic and cathodic peaks with large peak-to-peak displacement. Little improvement is observed in solutions of $Mg(BF_4)_2$ in propylene carbonate. No cathodic current is observed in this system, and voltage overload occurs with anodic current densities of only 40 ma/cm^2.

h. Nickel Chloride Electrode

Nickel chloride in dimethylformamide-$LiPF_6$ shows low order anodic and cathodic currents but no peak formation. No cathode currents are observed for acetonitrile and propylene carbonate solutions of $LiPF_6$. Multiple anodic peaks with current densities less than 25 ma/cm^2 occur in the acetonitrile solution, and less than 3 ma/cm^2 in propylene carbonate solution.

i. Nickel Fluoride Electrode

NiF_2 gives anodic voltage overload in BF_3 solutions of acetonitrile and butyrolactone. Negligible discharge current is indicated. Propylene carbonate-BF_3 solution, on the other hand, shows no electrode activity at all, with current densities less than 0.1 ma/cm^2/cm recorder deflection. Medium low charge currents are obtained in dimethylformamide-BF_3, but are very erratic at all sweep rates. Again, no discharge current is evident. The behavior of NiF_2 electrodes in $Mg(BF_4)_2$ and PF_5 solutions of acetonitrile, dimethylformamide, and propylene carbonate is generally poor, exhibiting little or no cathodic activity. The anodic sweeps show low peak current densities with the exception of the acetonitrile-$Mg(BF_4)_2$ system which exhibits erratic anodic peaks ranging from 60 to 150 ma/cm^2.

j. Cobalt Electrode

No discharge currents are observed with cobalt in acetonitrile and dimethylformamide solutions of $LiBF_4$, although very high anodic current densities of 1400 and 400 ma/cm^2 respectively are obtained. Discoloration of the solutions occurs in both cases. Cobalt in propylene carbonate-$Mg(BF_4)_2$ solution causes voltage overload for both anodic and cathodic sweeps with maximum current densities recorded at 40 ma/cm^2.

k. Cobalt Chloride Electrode

Medium low anodic and cathodic currents are obtained in dimethylformamide-$LiPF_6$ but only at the extreme charge and discharge potentials. Similar results are obtained in acetonitrile and propylene carbonate solutions of $LiPF_6$. These also compare with the data for cobalt metal. The cyclic voltammogram for $CoCl_3$ in dimethylformamide-$LiPF_6$ is shown in Figure 32 (CV-2310).

1. Cobalt Fluoride Electrode

Cobalt fluoride shows essentially no anodic or cathodic activity in all systems screened. Identical results were obtained for other solutions measured earlier (Ref. 2.).

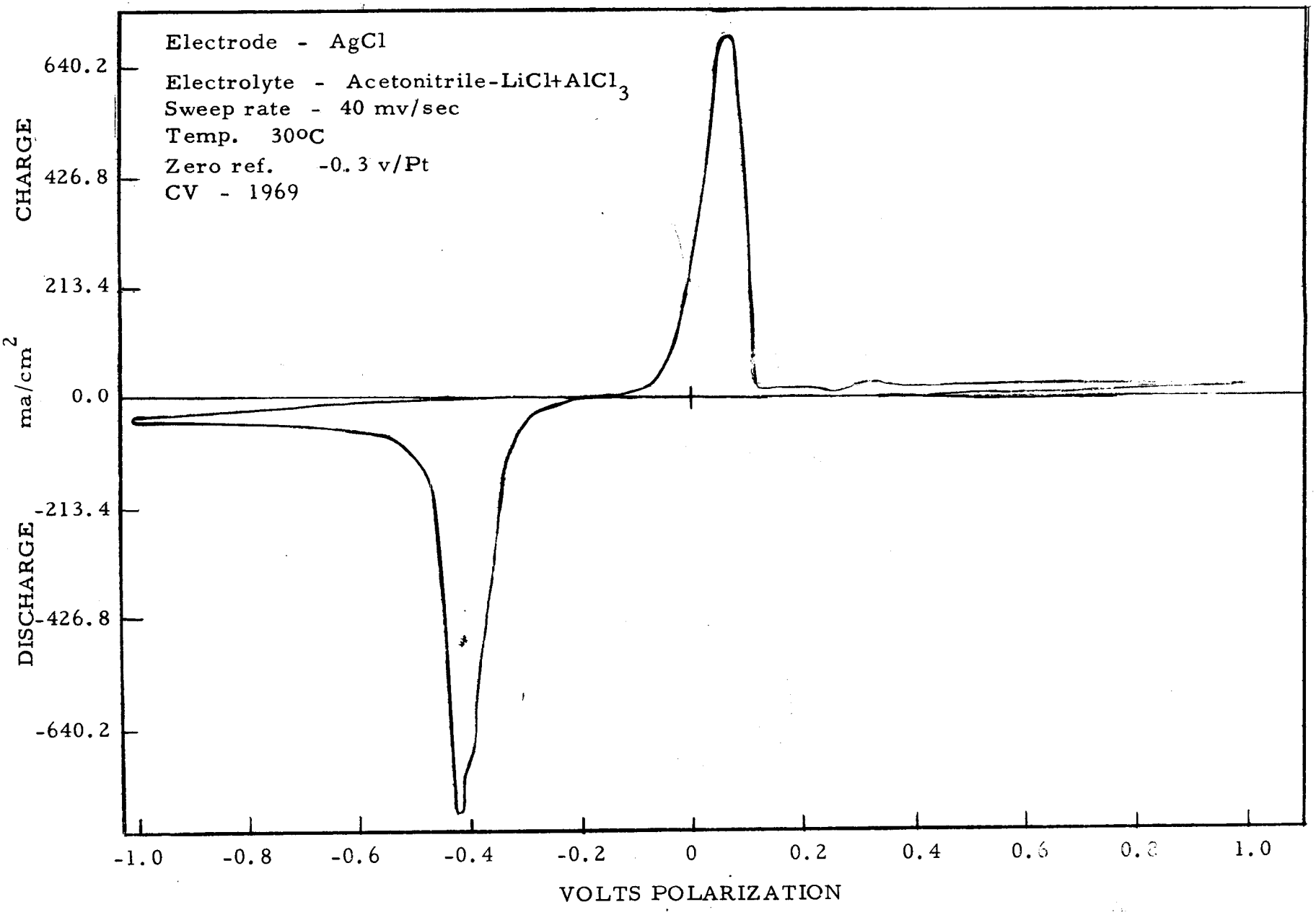
Electrode - AgCl
Electrolyte - Acetonitrile-LiCl+AlCl3
Sweep rate - 40 mv/sec
Temp. 30°C
Zero ref. -0.3 v/Pt
CV - 1969
CHARGE
DISCHARGE
ma/cm2
640.2
426.8
213.4
0.0
-213.4
-426.8
-640.2
-1.0
-0.8
-0.6
-0.4
-0.2
0
0.2
0.4
0.6
0.8
1.0
VOLTS POLARIZATION

Figure 1

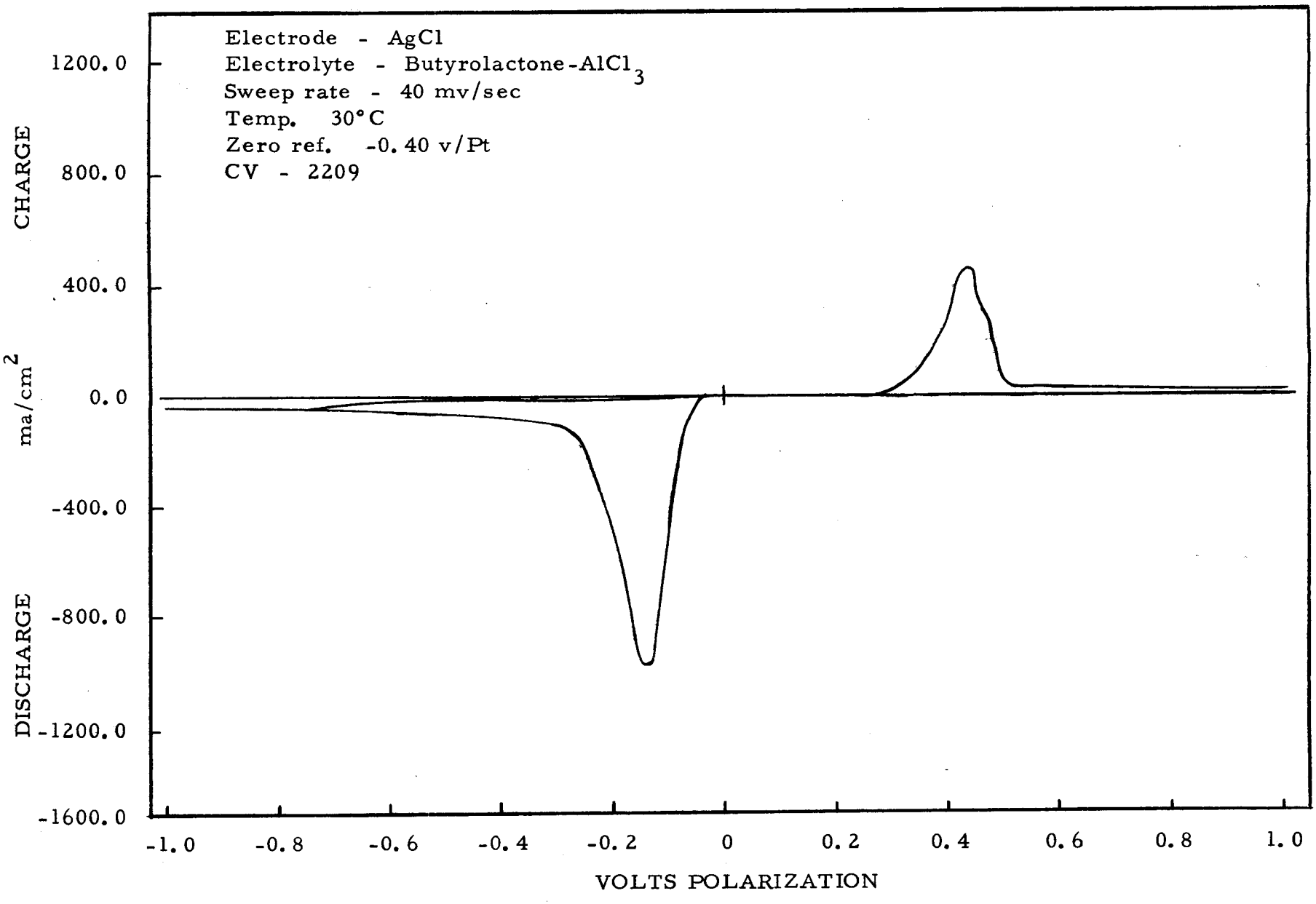
Electrode - AgCl
Electrolyte - Butyrolactone-AlCl3
Sweep rate - 40 mv/sec
Temp. 30°C
Zero ref. -0.40 v/Pt
CV - 2209
CHARGE
DISCHARGE
ma/cm2
1200.0
800.0
400.0
0.0
-400.0
-800.0
-1200.0
-1600.0
-1.0
-0.8
-0.6
-0.4
-0.2
0
0.2
0.4
0.6
0.8
1.0
VOLTS POLARIZATION

Figure 2

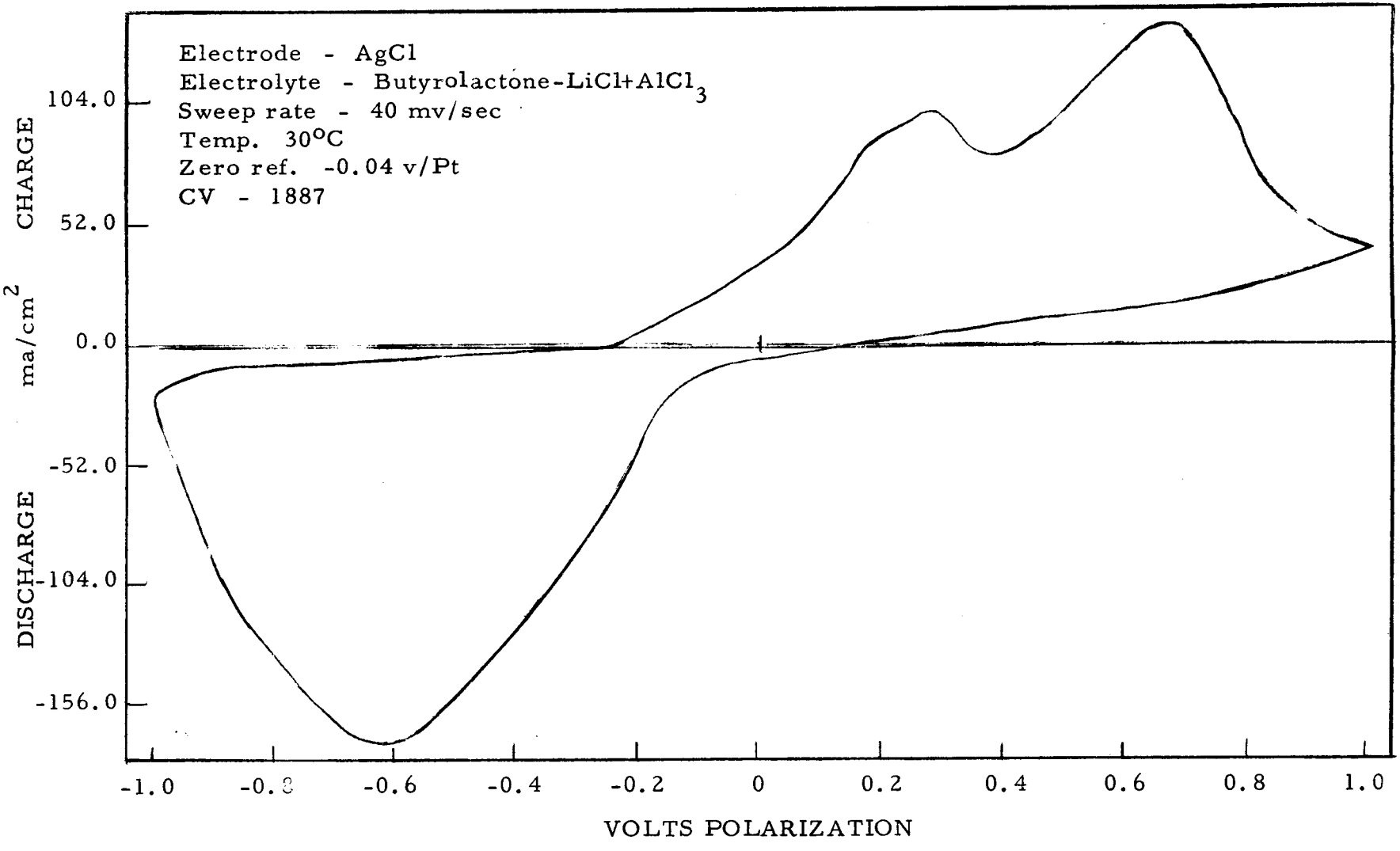
Electrode - AgCl
Electrolyte - Butyrolactone-LiCl+AlCl3
Sweep rate - 40 mv/sec
Temp. 30°C
Zero ref. -0.04 v/Pt
CV - 1887
CHARGE
DISCHARGE
ma/cm2
104.0
52.0
0.0
-52.0
-104.0
-156.0
-1.0
-0.8
-0.6
-0.4
-0.2
0
0.2
0.4
0.6
0.8
1.0
VOLTS POLARIZATION

Figure 3

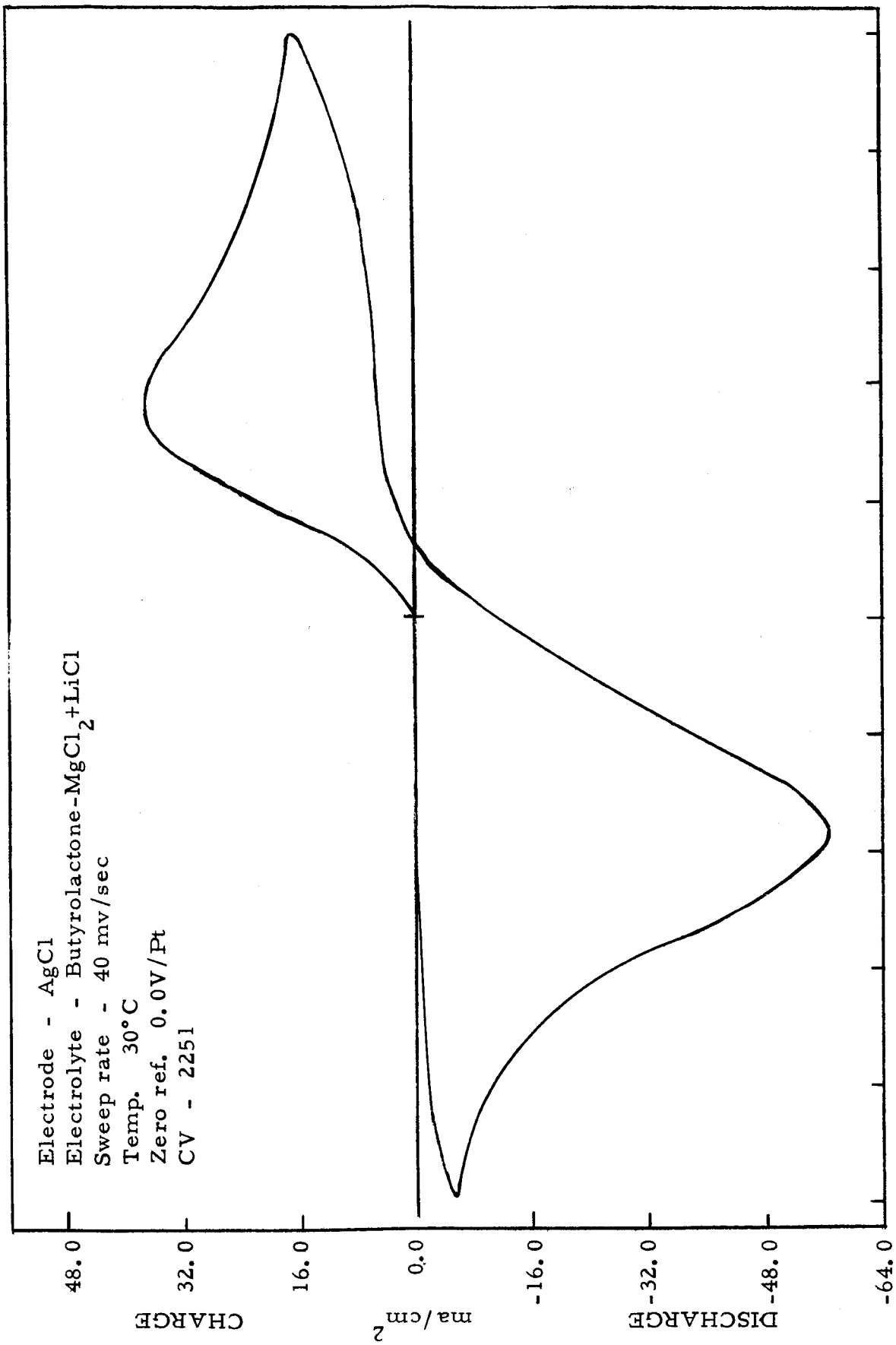
Electrode - AgCl
Electrolyte - Butyrolactone-$MgCl_2$+LiCl
Sweep rate - 40 mv/sec
Temp. 30°C
Zero ref. 0.0V/Pt
CV - 2251
48.0
32.0
16.0
0.0
-16.0
-32.0
-48.0
-64.0
CHARGE
DISCHARGE
ma/cm^2
-1.0
-0.8
-0.6
-0.4
-0.2
0
0.2
0.4
0.6
0.8
1.0
VOLTS POLARIZATION

Figure 4

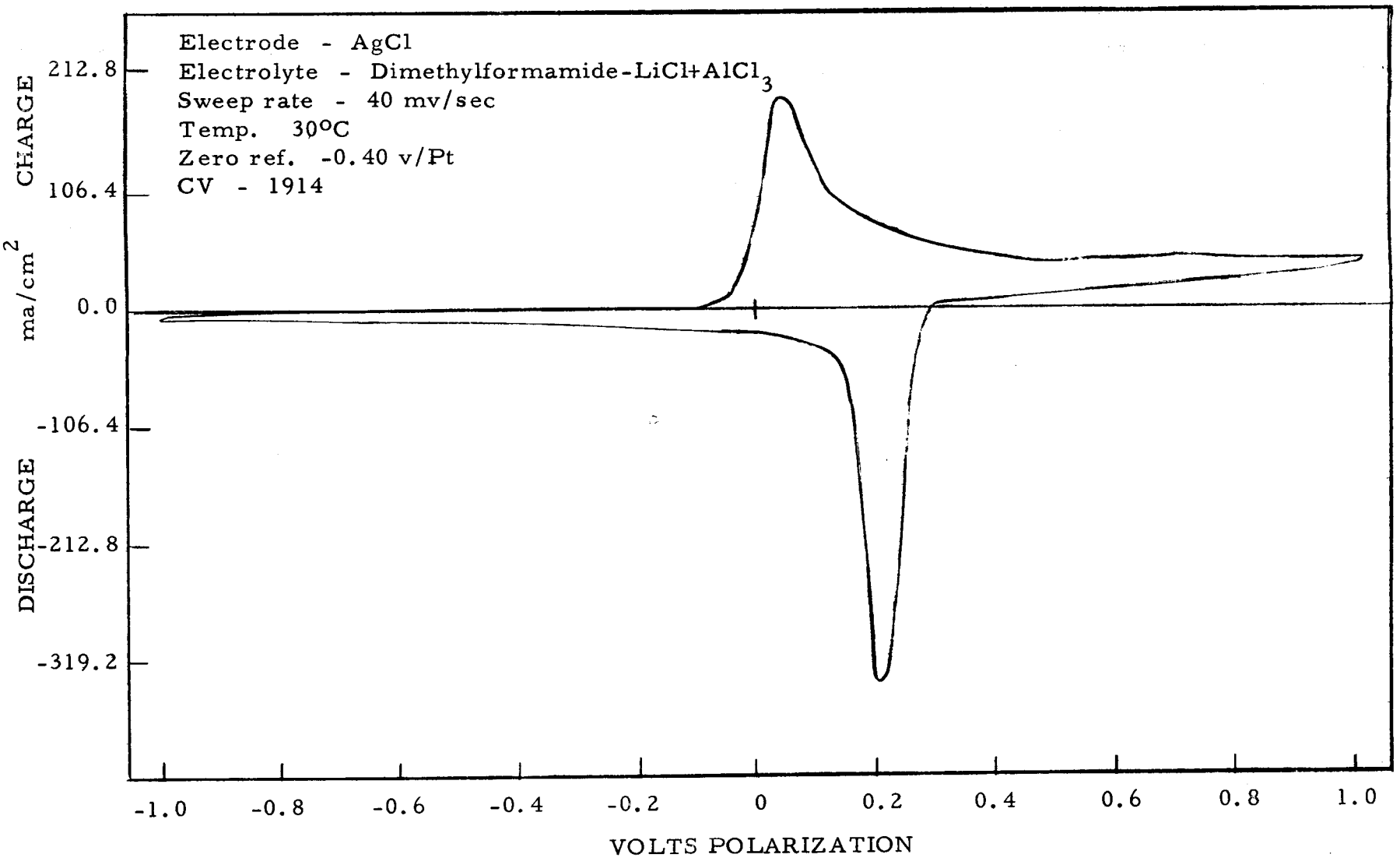
Electrode - AgCl
Electrolyte - Dimethylformamide-LiCl+AlCl3
Sweep rate - 40 mv/sec
Temp. 30°C
Zero ref. -0.40 v/Pt
CV - 1914
CHARGE
DISCHARGE
ma/cm2
212.8
106.4
0.0
-106.4
-212.8
-319.2
-1.0
-0.8
-0.6
-0.4
-0.2
0
0.2
0.4
0.6
0.8
1.0
VOLTS POLARIZATION

Figure 5

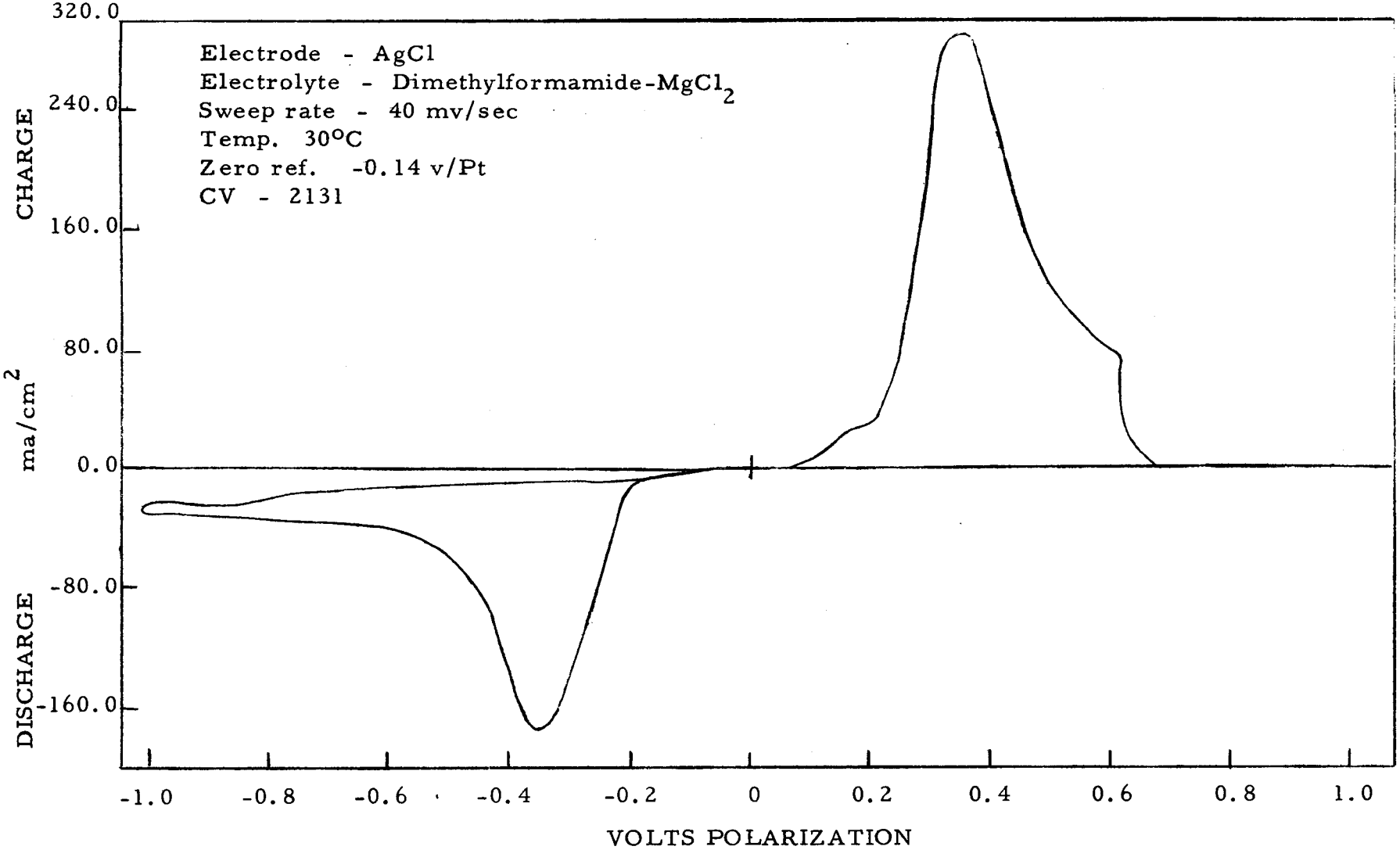
Electrode - AgCl
Electrolyte - Dimethylformamide-$MgCl_2$
Sweep rate - 40 mv/sec
Temp. 30°C
Zero ref. -0.14 v/Pt
CV - 2131
320.0
240.0
160.0
80.0
0.0
-80.0
-160.0
CHARGE
DISCHARGE
ma/cm^2
-1.0
-0.8
-0.6
-0.4
-0.2
0
0.2
0.4
0.6
0.8
1.0
VOLTS POLARIZATION

Figure 6

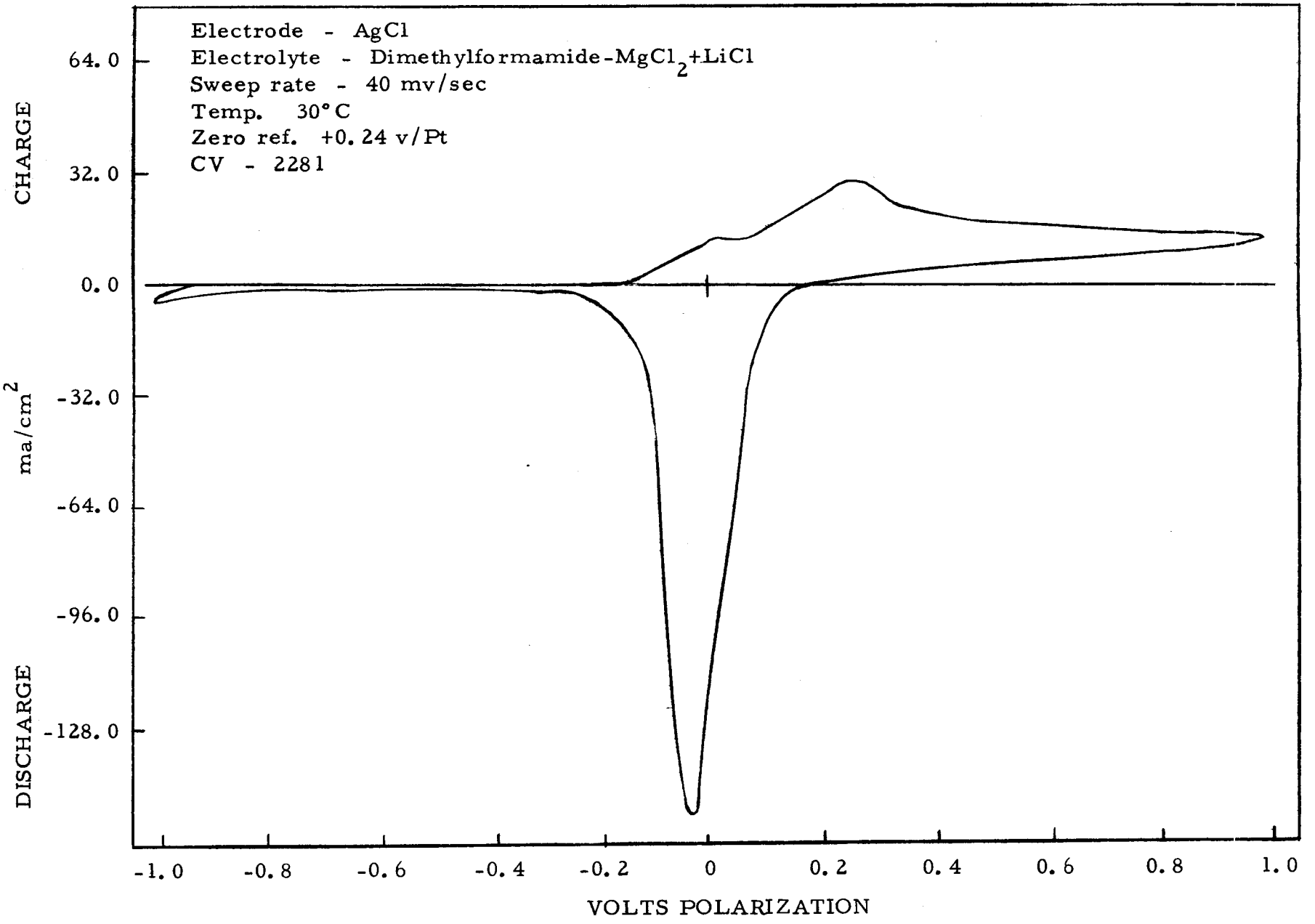
Electrode - AgCl
Electrolyte - Dimethylformamide-$MgCl_2$+LiCl
Sweep rate - 40 mv/sec
Temp. 30°C
Zero ref. +0.24 v/Pt
CV - 2281
CHARGE
DISCHARGE
ma/cm^2
64.0
32.0
0.0
-32.0
-64.0
-96.0
-128.0
-1.0
-0.8
-0.6
-0.4
-0.2
0
0.2
0.4
0.6
0.8
1.0
VOLTS POLARIZATION

Figure 7

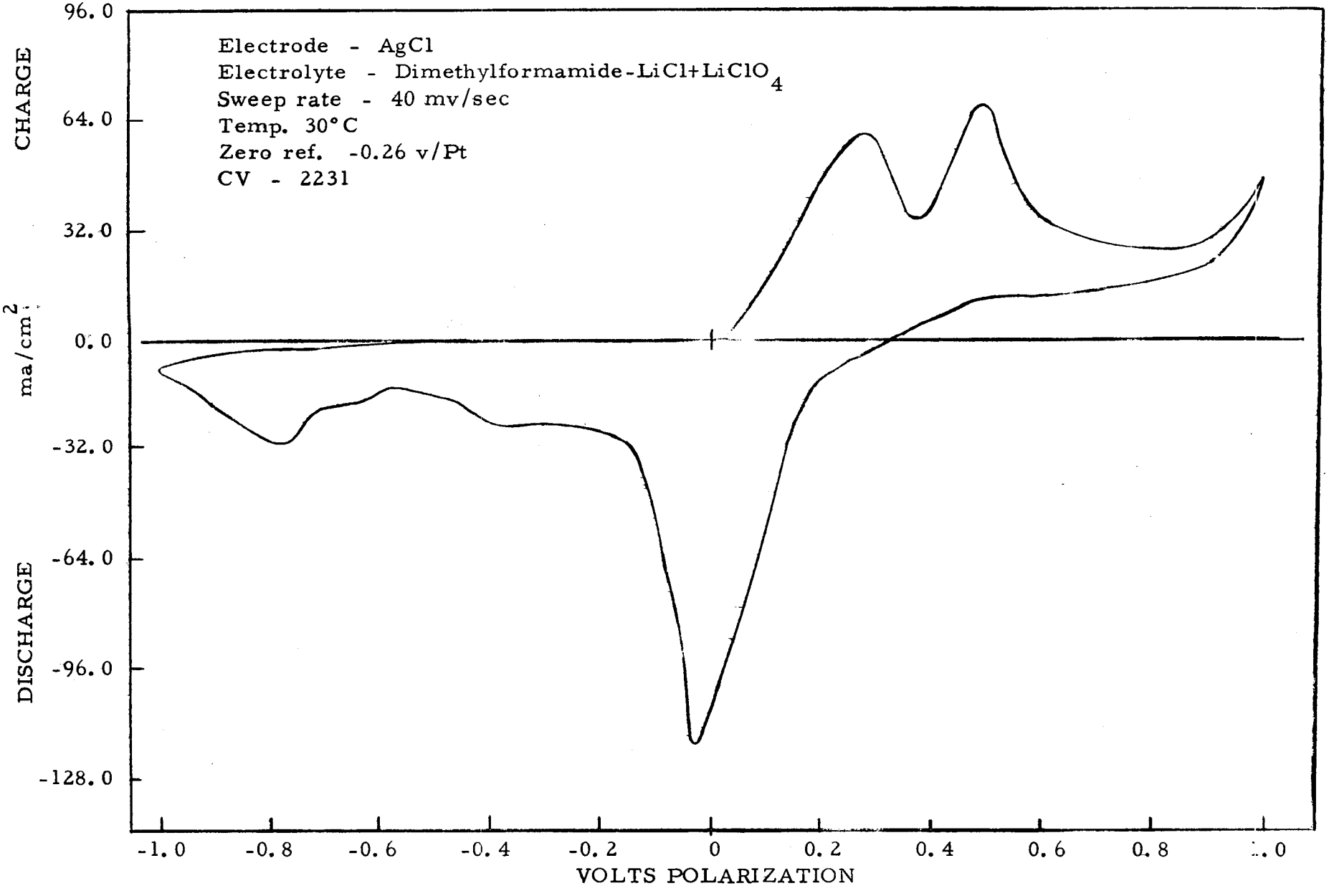
Electrode - AgCl
Electrolyte - Dimethylformamide-LiCl+LiClO4
Sweep rate - 40 mv/sec
Temp. 30°C
Zero ref. -0.26 v/Pt
CV - 2231
CHARGE
DISCHARGE
ma/cm2
96.0
64.0
32.0
0.0
-32.0
-64.0
-96.0
-128.0
-1.0
-0.8
-0.6
-0.4
-0.2
0
0.2
0.4
0.6
0.8
1.0
VOLTS POLARIZATION

Figure 8

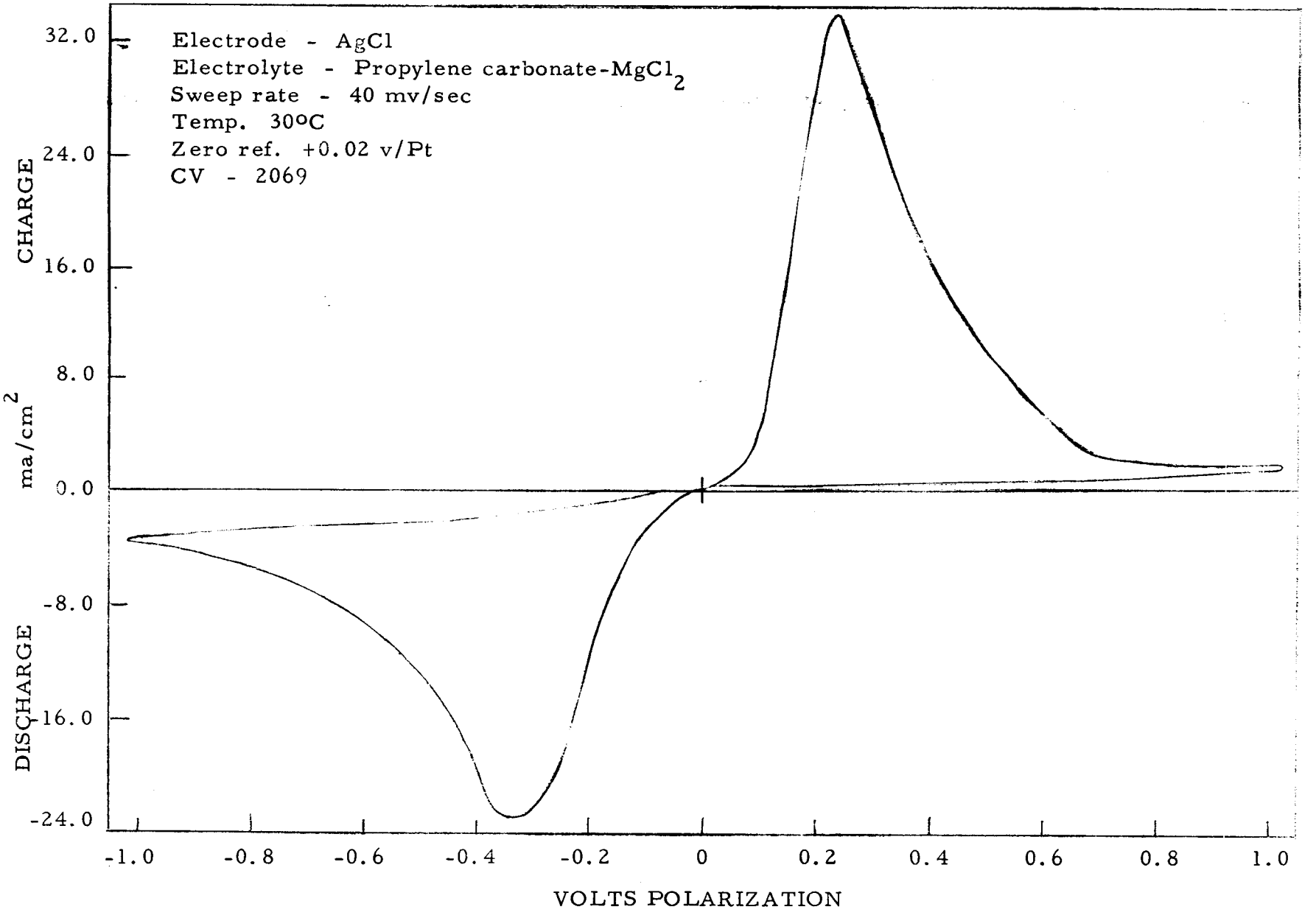
Electrode - AgCl
Electrolyte - Propylene carbonate-$MgCl_2$
Sweep rate - 40 mv/sec
Temp. 30°C
Zero ref. +0.02 v/Pt
CV - 2069
CHARGE
DISCHARGE
ma/cm^2
32.0
24.0
16.0
8.0
0.0
-8.0
-16.0
-24.0
-1.0
-0.8
-0.6
-0.4
-0.2
0
0.2
0.4
0.6
0.8
1.0
VOLTS POLARIZATION

Figure 9

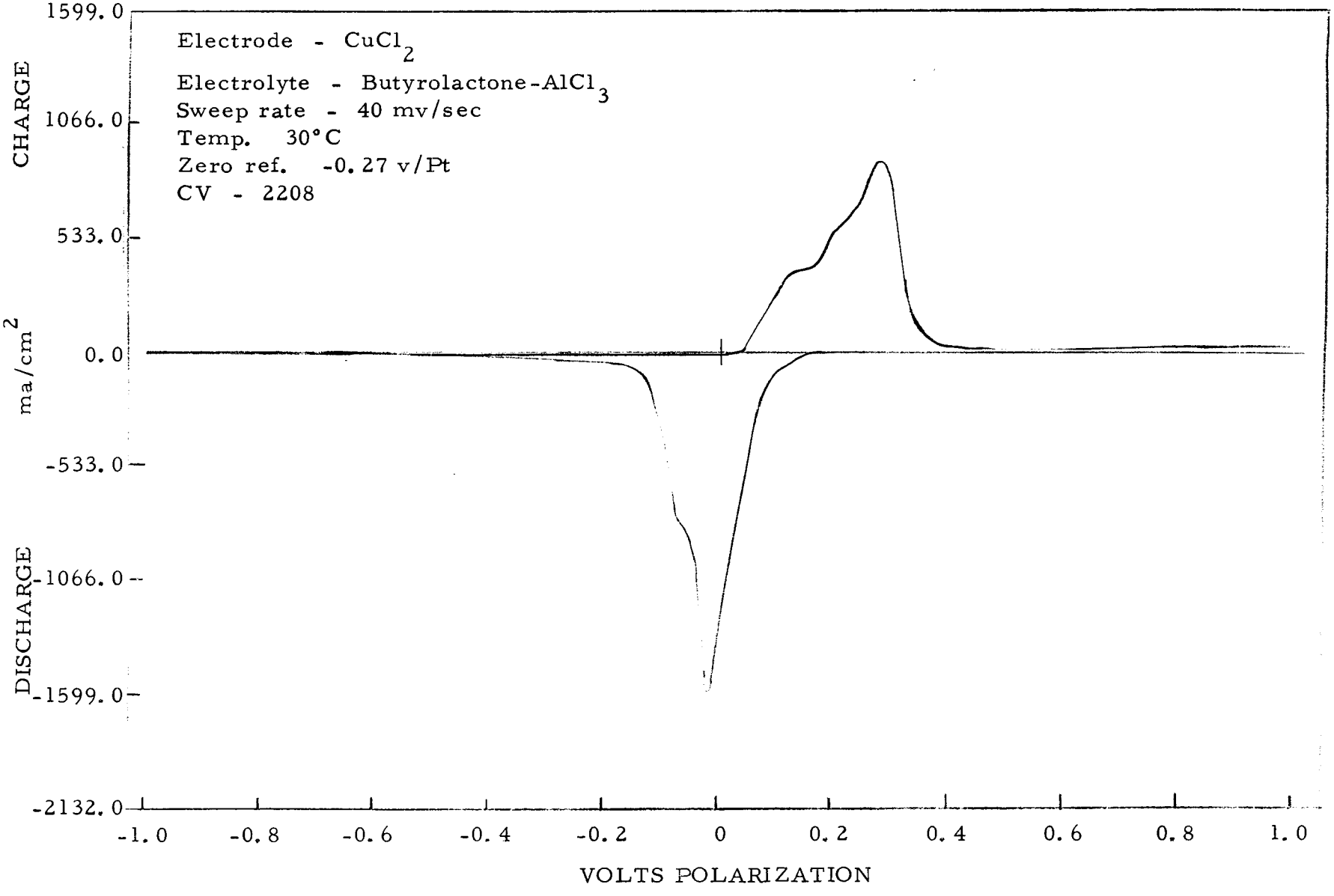
Electrode - $CuCl_2$
Electrolyte - Butyrolactone-$AlCl_3$
Sweep rate - 40 mv/sec
Temp. 30°C
Zero ref. -0.27 v/Pt
CV - 2208
CHARGE
DISCHARGE
ma/cm^2
1599.0
1066.0
533.0
0.0
-533.0
-1066.0
-1599.0
-2132.0
-1.0
-0.8
-0.6
-0.4
-0.2
0
0.2
0.4
0.6
0.8
1.0
VOLTS POLARIZATION

Figure 10

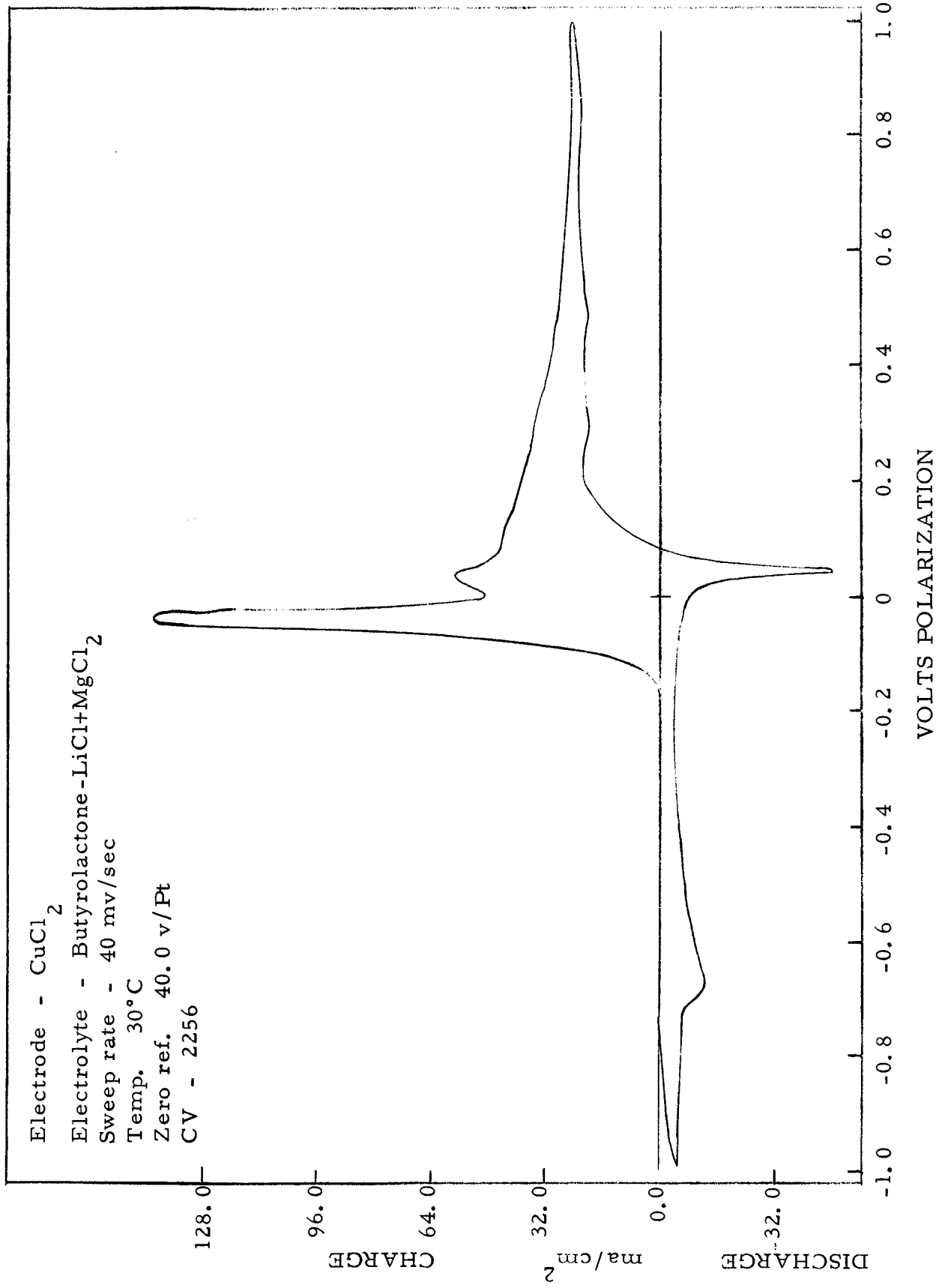
Electrode - $CuCl_2$
Electrolyte - Butyrolactone-LiCl+$MgCl_2$
Sweep rate - 40 mv/sec
Temp. 30°C
Zero ref. 40.0 v/Pt
CV - 2256
128.0
96.0
64.0
32.0
0.0
-32.0
CHARGE
DISCHARGE
ma/cm^2
-1.0
-0.8
-0.6
-0.4
-0.2
0
0.2
0.4
0.6
0.8
1.0
VOLTS POLARIZATION

Figure 11

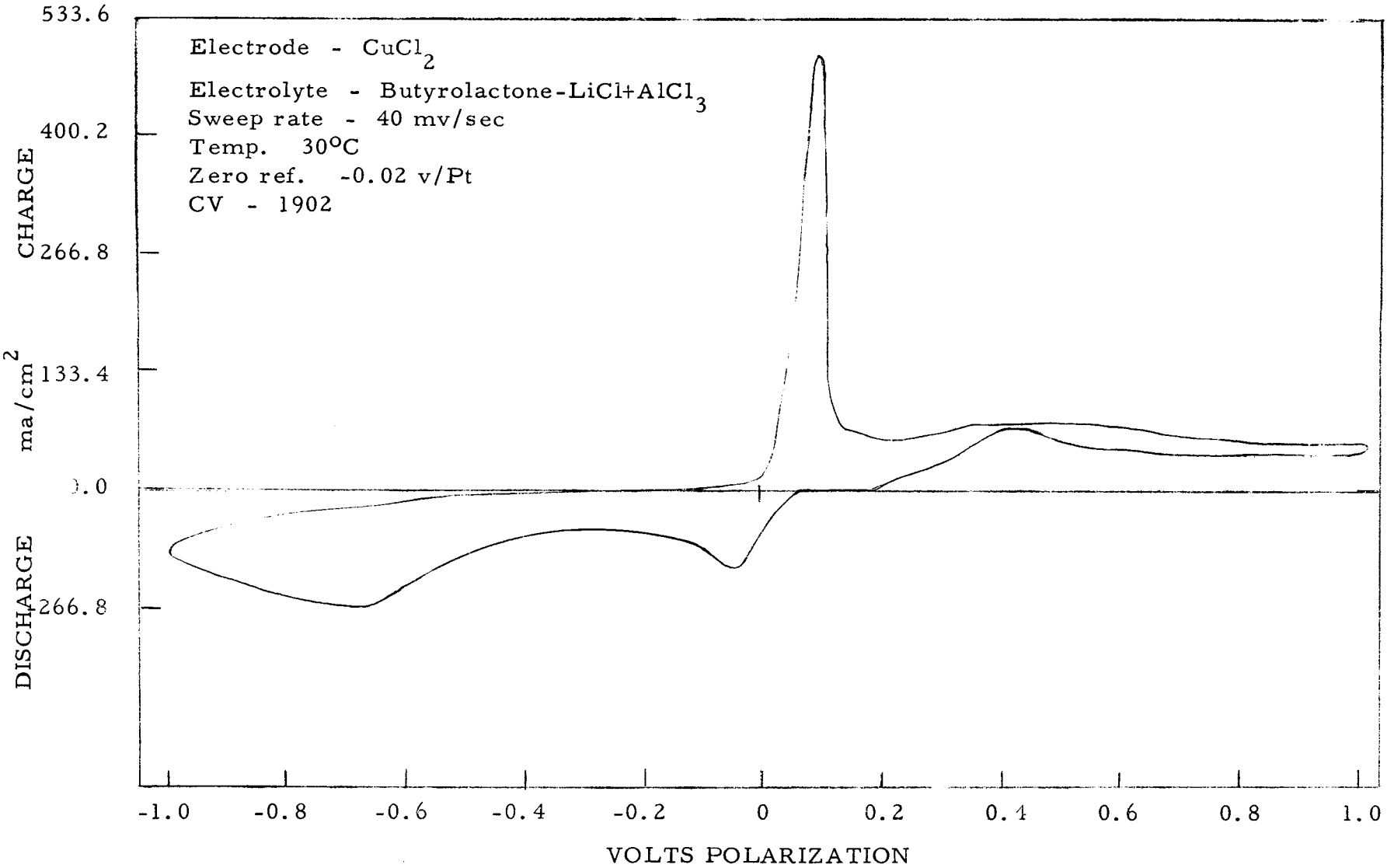
Electrode - $CuCl_2$
Electrolyte - Butyrolactone-$LiCl+AlCl_3$
Sweep rate - 40 mv/sec
Temp. 30°C
Zero ref. -0.02 v/Pt
CV - 1902
533.6
400.2
266.8
133.4
0.0
266.8
CHARGE
DISCHARGE
ma/cm^2
-1.0
-0.8
-0.6
-0.4
-0.2
0
0.2
0.4
0.6
0.8
1.0
VOLTS POLARIZATION

Figure 12

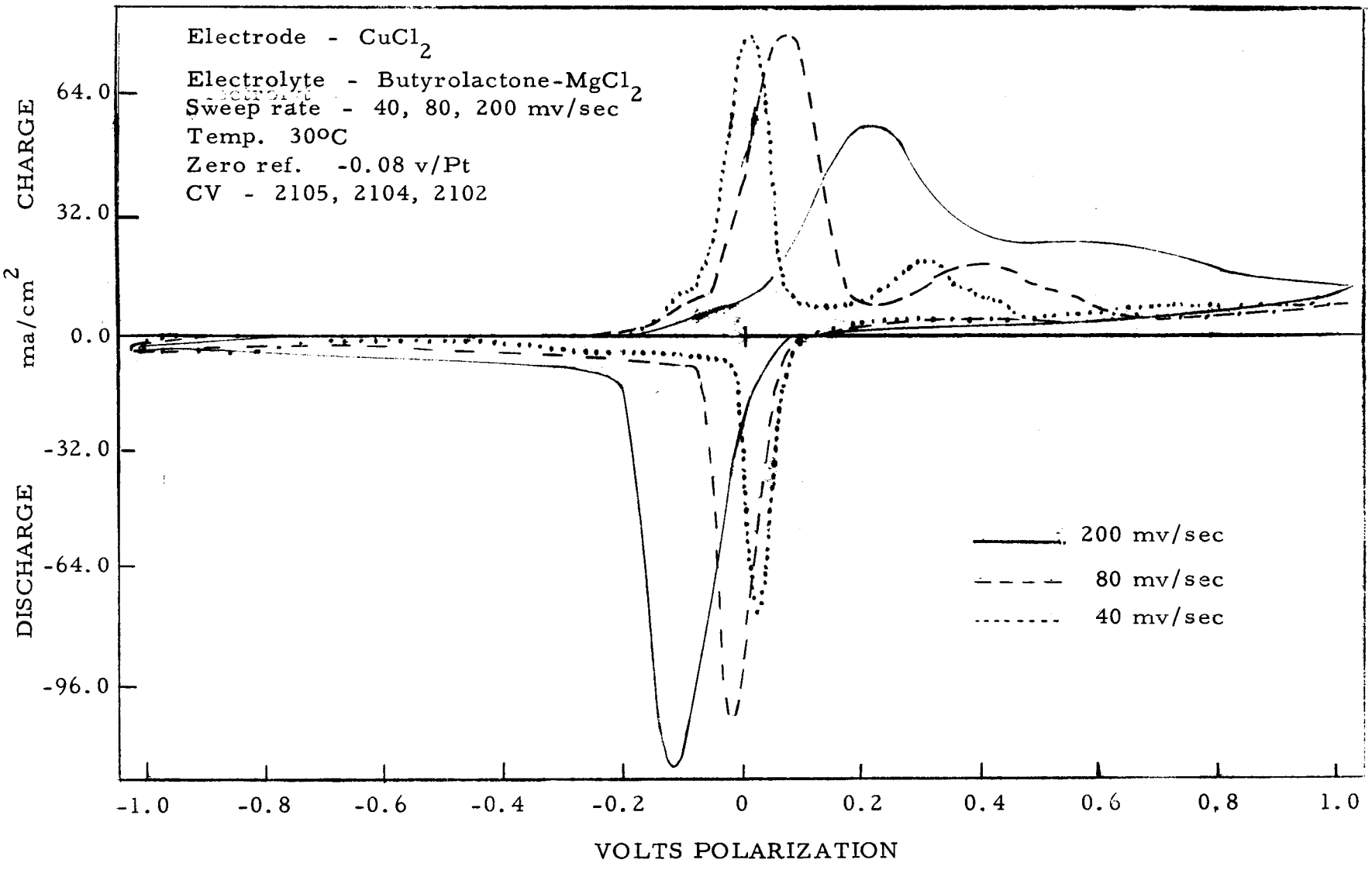
Electrode - $CuCl_2$
Electrolyte - Butyrolactone-$MgCl_2$
Sweep rate - 40, 80, 200 mv/sec
Temp. 30°C
Zero ref. -0.08 v/Pt
CV - 2105, 2104, 2102
CHARGE
DISCHARGE
ma/cm^2
64.0
32.0
0.0
-32.0
-64.0
-96.0
200 mv/sec
80 mv/sec
40 mv/sec
-1.0
-0.8
-0.6
-0.4
-0.2
0
0.2
0.4
0.6
0.8
1.0
VOLTS POLARIZATION

Figure 13

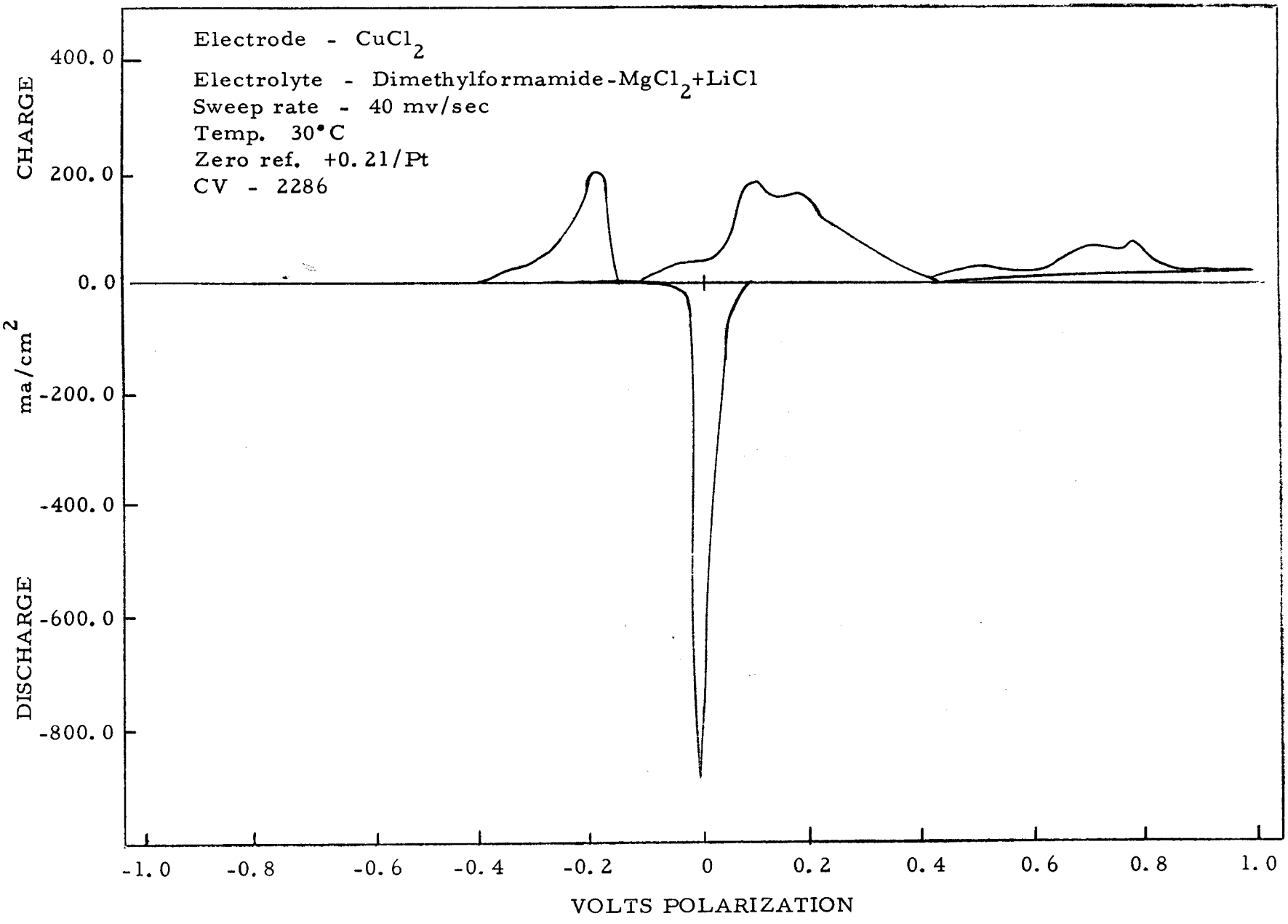
Electrode - $CuCl_2$
Electrolyte - Dimethylformamide-$MgCl_2$+LiCl
Sweep rate - 40 mv/sec
Temp. 30°C
Zero ref. +0.21/Pt
CV - 2286
CHARGE
DISCHARGE
ma/cm^2
400.0
200.0
0.0
-200.0
-400.0
-600.0
-800.0
-1.0
-0.8
-0.6
-0.4
-0.2
0
0.2
0.4
0.6
0.8
1.0
VOLTS POLARIZATION

Figure 14

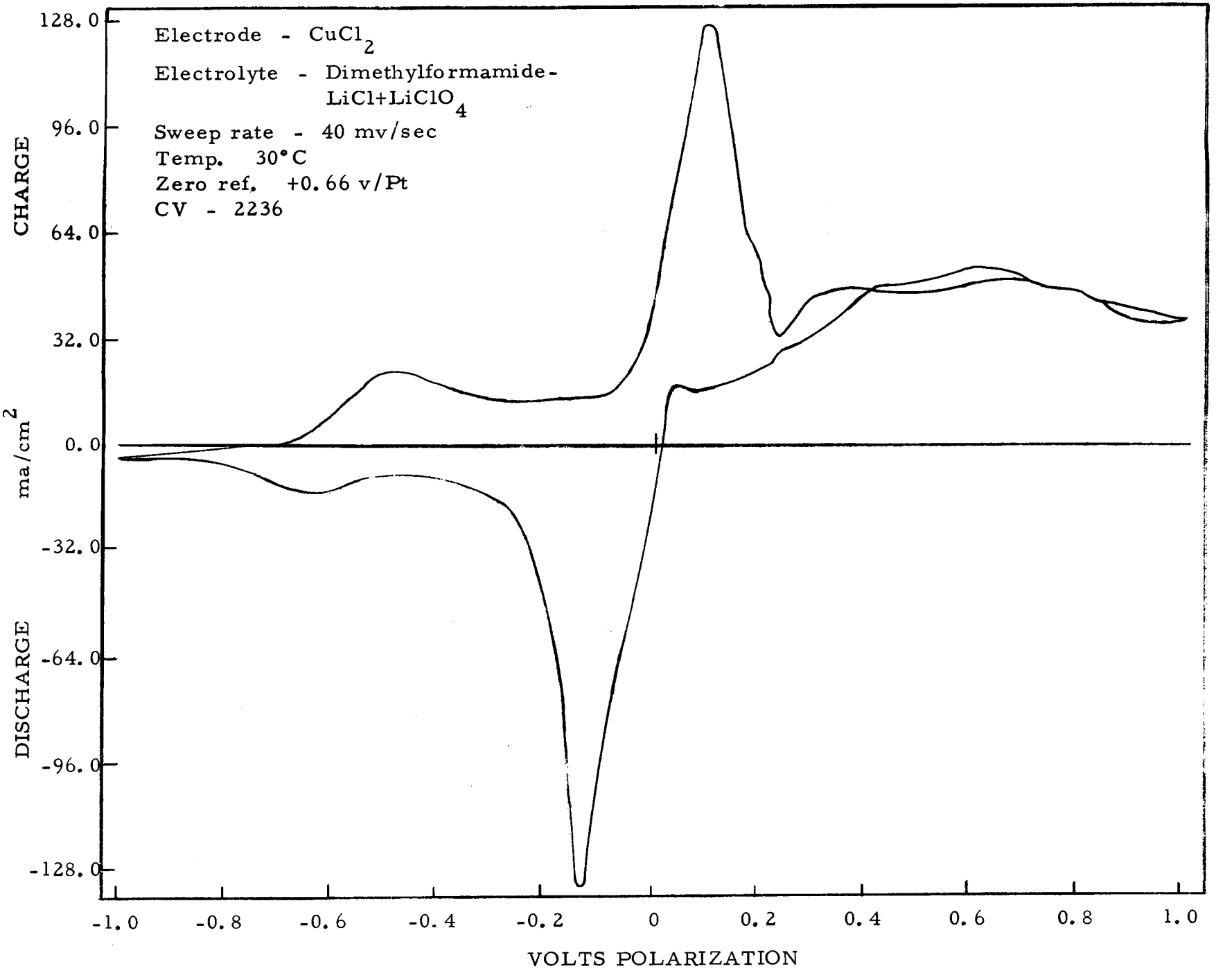
Electrode - $CuCl_2$
Electrolyte - Dimethylformamide-$LiCl+LiClO_4$
Sweep rate - 40 mv/sec
Temp. 30°C
Zero ref. +0.66 v/Pt
CV - 2236
CHARGE
DISCHARGE
ma/cm^2
128.0
96.0
64.0
32.0
0.0
-32.0
-64.0
-96.0
-128.0
-1.0
-0.8
-0.6
-0.4
-0.2
0
0.2
0.4
0.6
0.8
1.0
VOLTS POLARIZATION

Figure 15

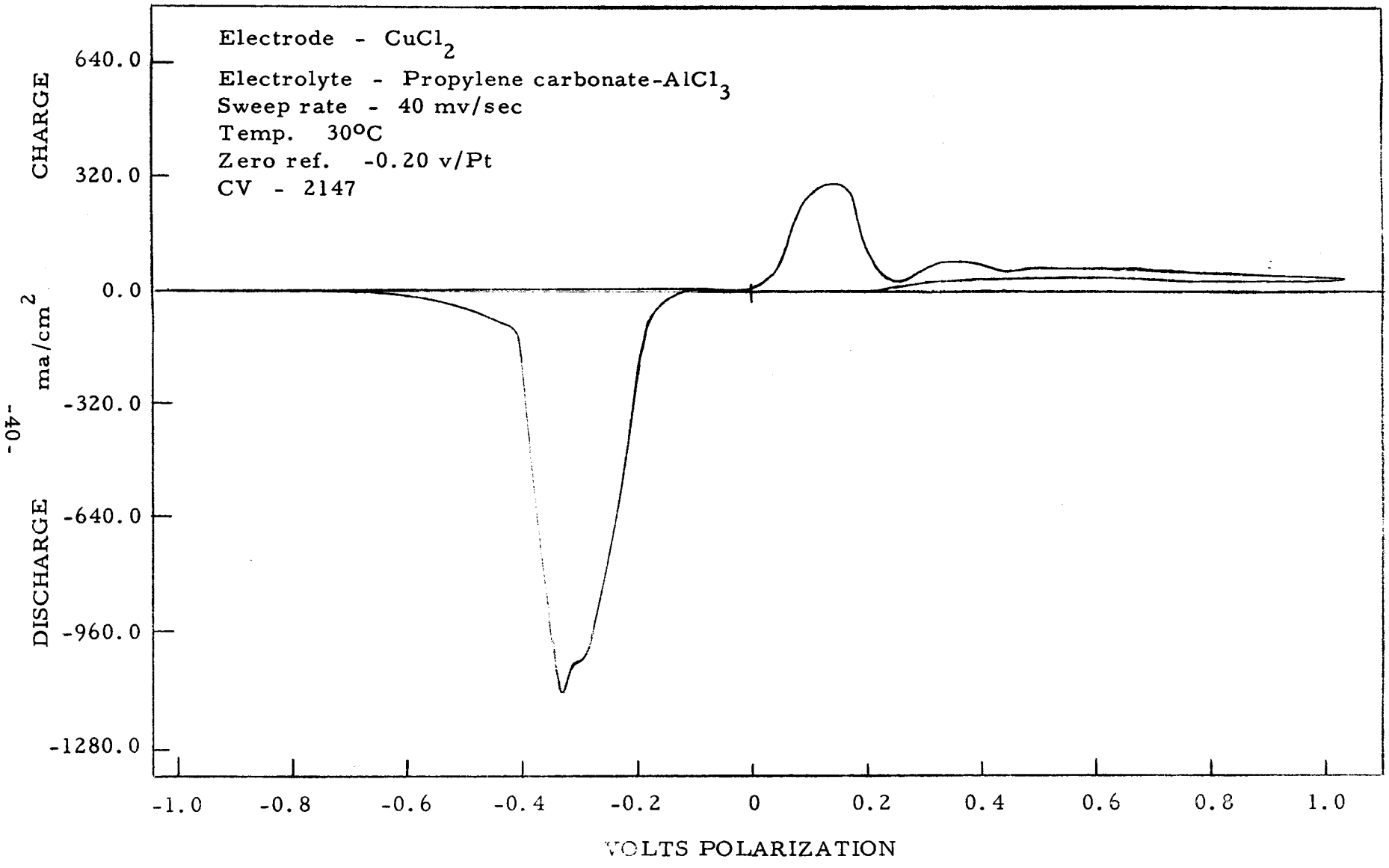
Electrode - $CuCl_2$
Electrolyte - Propylene carbonate-$AlCl_3$
Sweep rate - 40 mv/sec
Temp. 30°C
Zero ref. -0.20 v/Pt
CV - 2147
CHARGE
DISCHARGE
ma/cm^2
640.0
320.0
0.0
-320.0
-640.0
-960.0
-1280.0
-1.0
-0.8
-0.6
-0.4
-0.2
0
0.2
0.4
0.6
0.8
1.0
VOLTS POLARIZATION

Figure 16

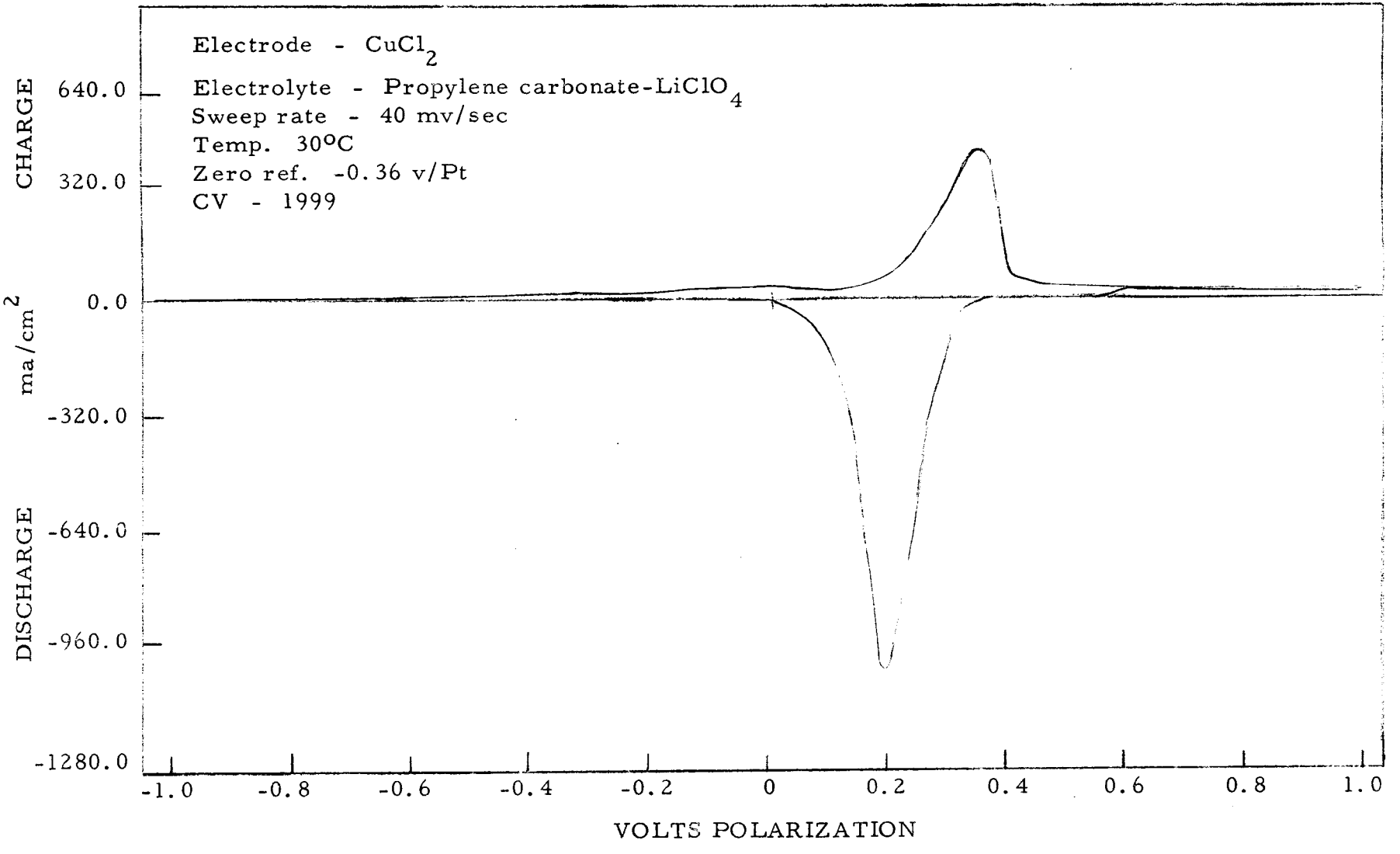
Electrode - $CuCl_2$
Electrolyte - Propylene carbonate-$LiClO_4$
Sweep rate - 40 mv/sec
Temp. 30°C
Zero ref. -0.36 v/Pt
CV - 1999
CHARGE
DISCHARGE
ma/cm^2
640.0
320.0
0.0
-320.0
-640.0
-960.0
-1280.0
-1.0
-0.8
-0.6
-0.4
-0.2
0
0.2
0.4
0.6
0.8
1.0
VOLTS POLARIZATION

Figure 17

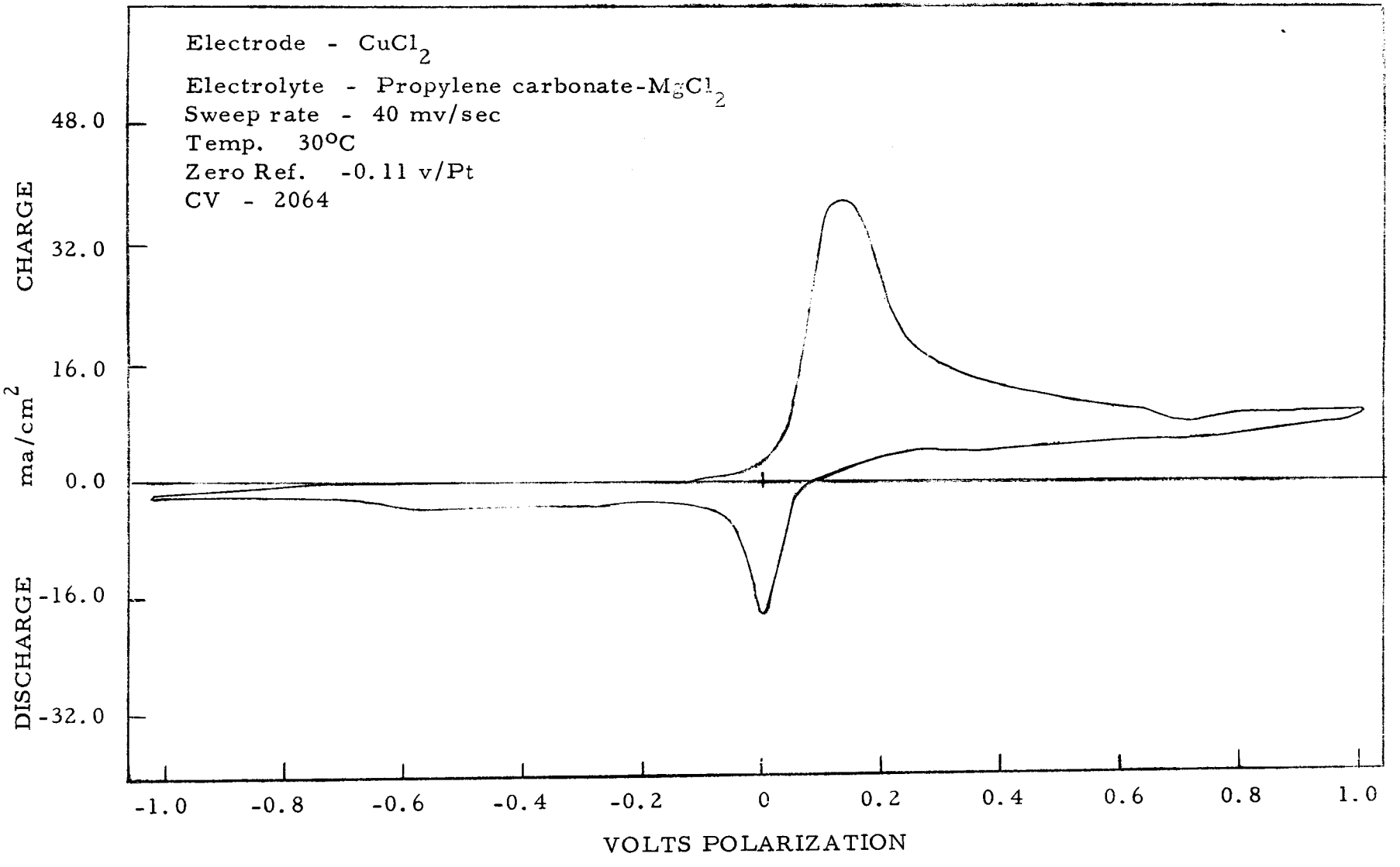
Electrode - $CuCl_2$
Electrolyte - Propylene carbonate-$MgCl_2$
Sweep rate - 40 mv/sec
Temp. 30°C
Zero Ref. -0.11 v/Pt
CV - 2064
48.0
32.0
16.0
0.0
-16.0
-32.0
CHARGE
DISCHARGE
ma/cm^2
-1.0
-0.8
-0.6
-0.4
-0.2
0
0.2
0.4
0.6
0.8
1.0
VOLTS POLARIZATION

Figure 18

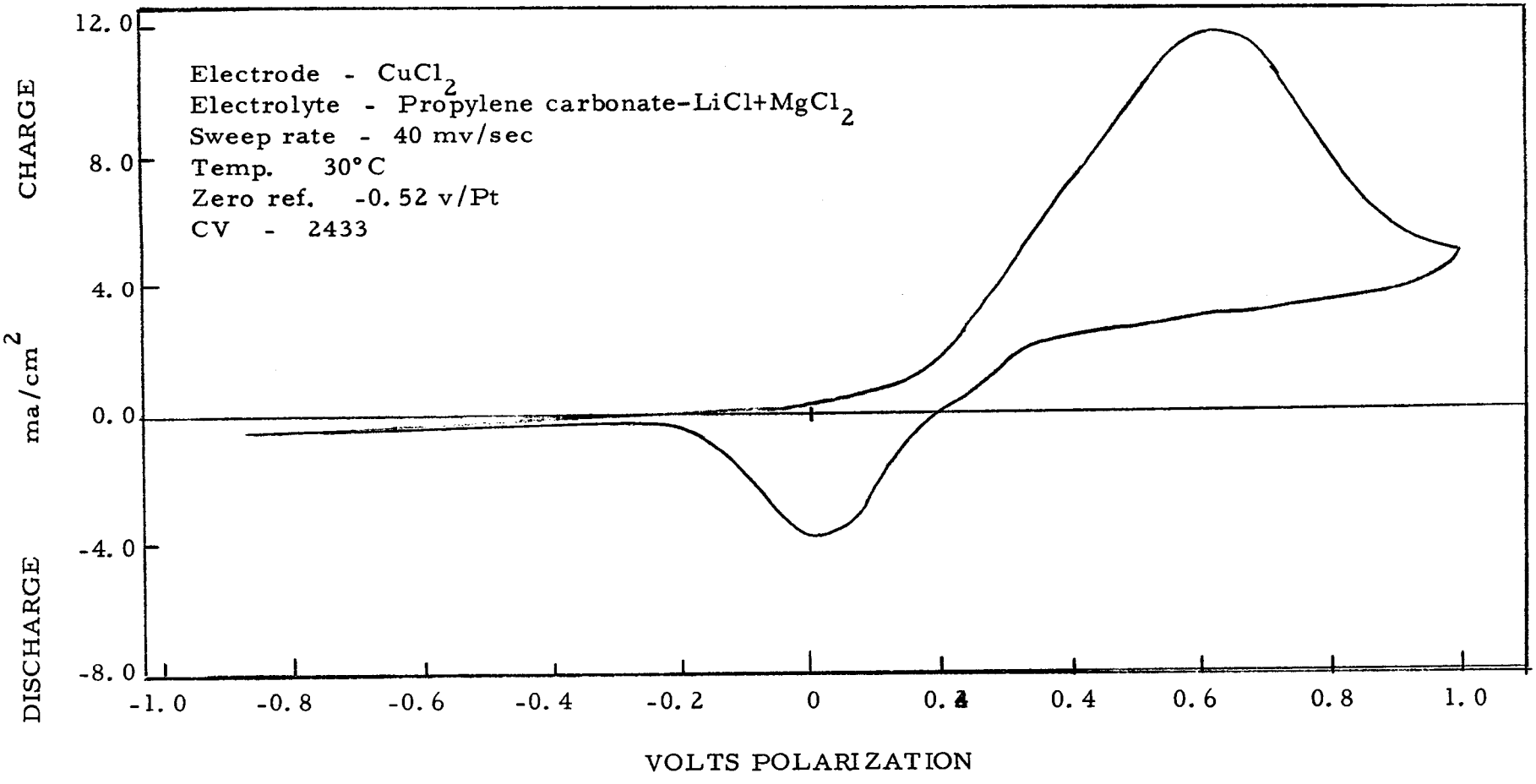
Electrode - $CuCl_2$
Electrolyte - Propylene carbonate-LiCl+$MgCl_2$
Sweep rate - 40 mv/sec
Temp. 30°C
Zero ref. -0.52 v/Pt
CV - 2433
CHARGE
DISCHARGE
ma/cm^2
12.0
8.0
4.0
0.0
-4.0
-8.0
-1.0
-0.8
-0.6
-0.4
-0.2
0
0.2
0.4
0.6
0.8
1.0
VOLTS POLARIZATION

Figure 19

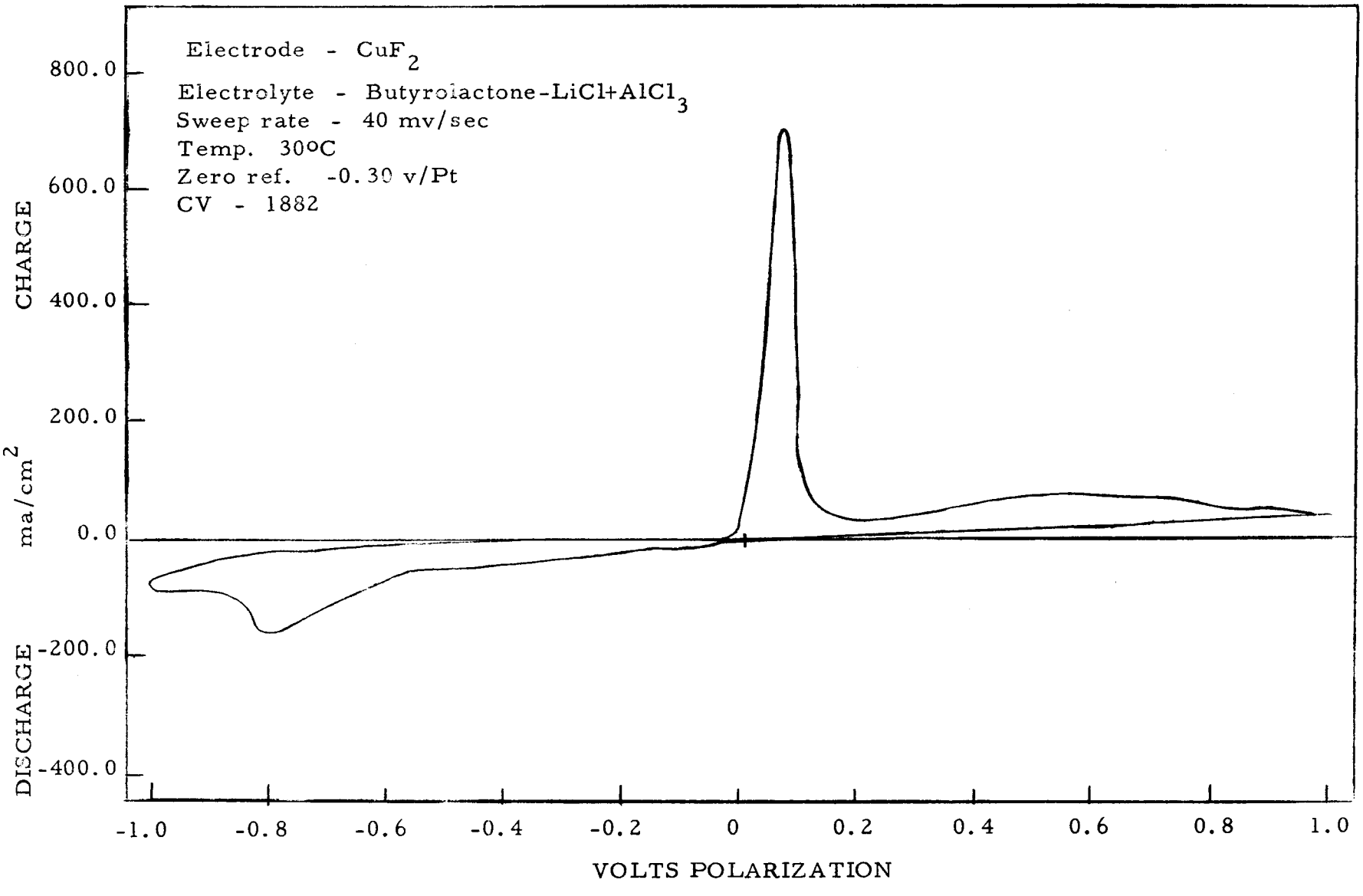
Electrode - CuF_2
Electrolyte - Butyrolactone-$LiCl+AlCl_3$
Sweep rate - 40 mv/sec
Temp. 30°C
Zero ref. -0.30 v/Pt
CV - 1882
800.0
600.0
400.0
200.0
0.0
-200.0
-400.0
CHARGE
DISCHARGE
ma/cm^2
-1.0
-0.8
-0.6
-0.4
-0.2
0
0.2
0.4
0.6
0.8
1.0
VOLTS POLARIZATION

Figure 20

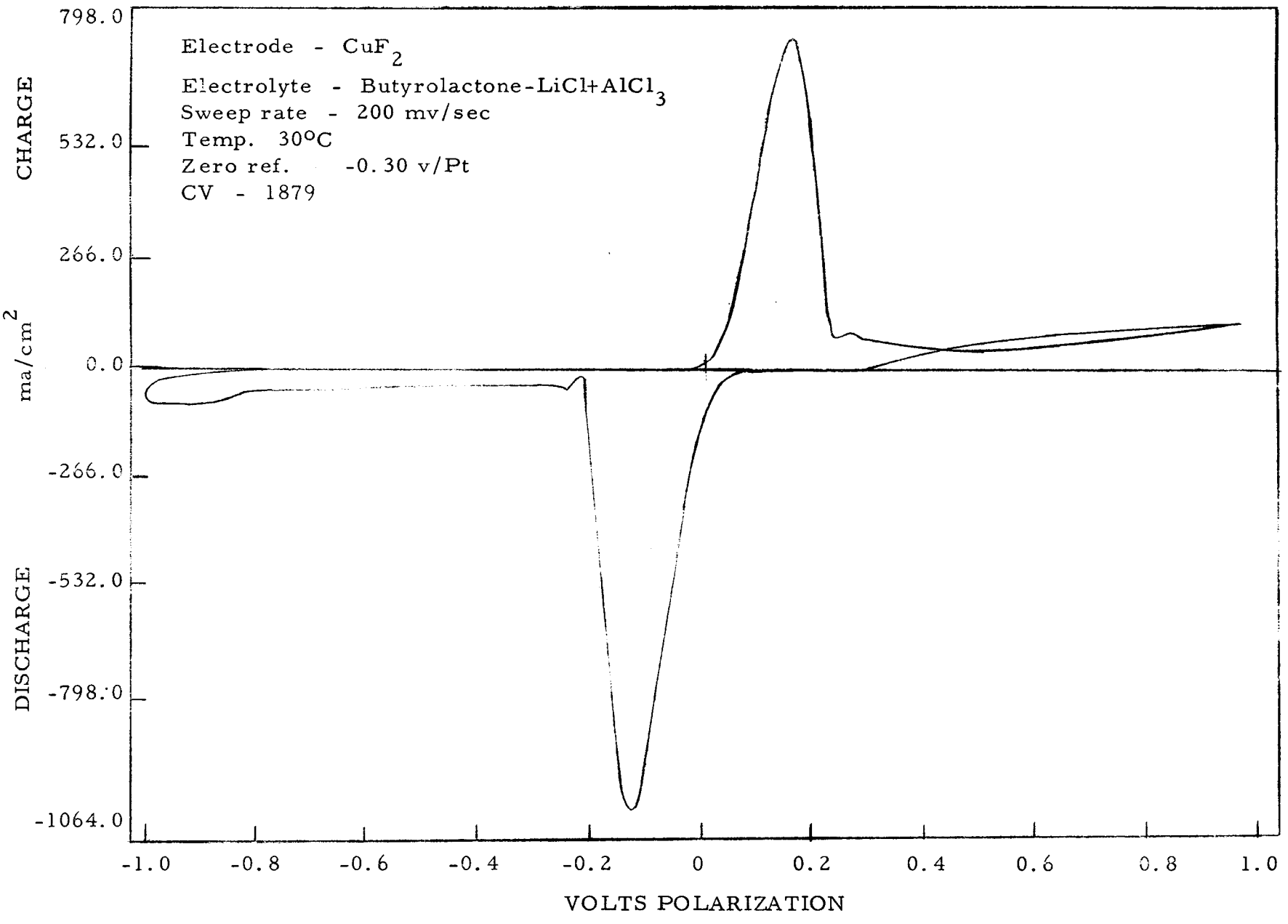
Electrode - CuF_2
Electrolyte - Butyrolactone-$LiCl+AlCl_3$
Sweep rate - 200 mv/sec
Temp. 30°C
Zero ref. -0.30 v/Pt
CV - 1879
798.0
532.0
266.0
0.0
-266.0
-532.0
-798.0
-1064.0
CHARGE
DISCHARGE
ma/cm^2
-1.0
-0.8
-0.6
-0.4
-0.2
0
0.2
0.4
0.6
0.8
1.0
VOLTS POLARIZATION

Figure 21

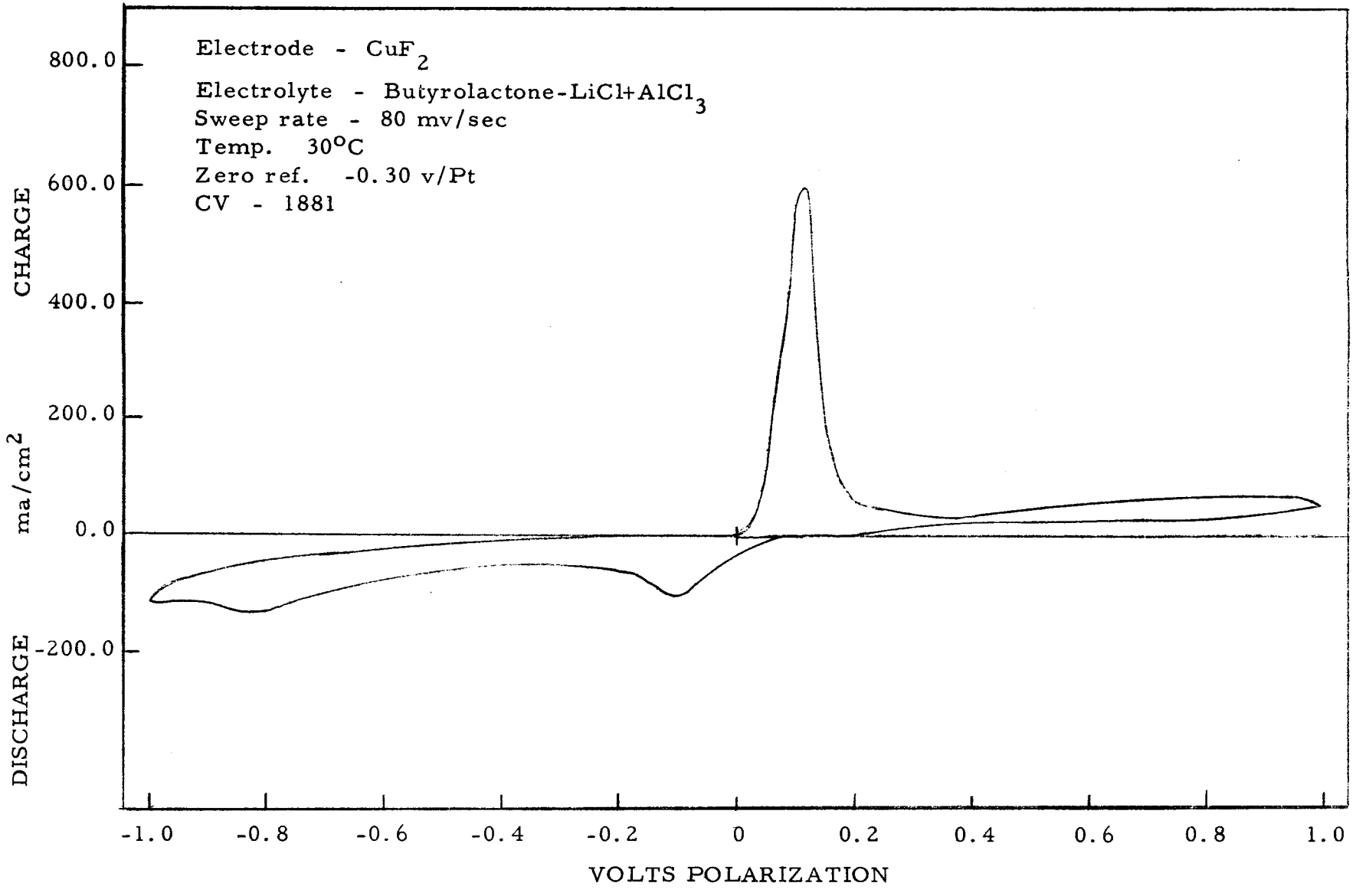
Electrode - CuF_2
Electrolyte - Butyrolactone-$LiCl+AlCl_3$
Sweep rate - 80 mv/sec
Temp. 30°C
Zero ref. -0.30 v/Pt
CV - 1881
800.0
600.0
400.0
200.0
0.0
-200.0
CHARGE
DISCHARGE
ma/cm²
-1.0
-0.8
-0.6
-0.4
-0.2
0
0.2
0.4
0.6
0.8
1.0
VOLTS POLARIZATION

Figure 22

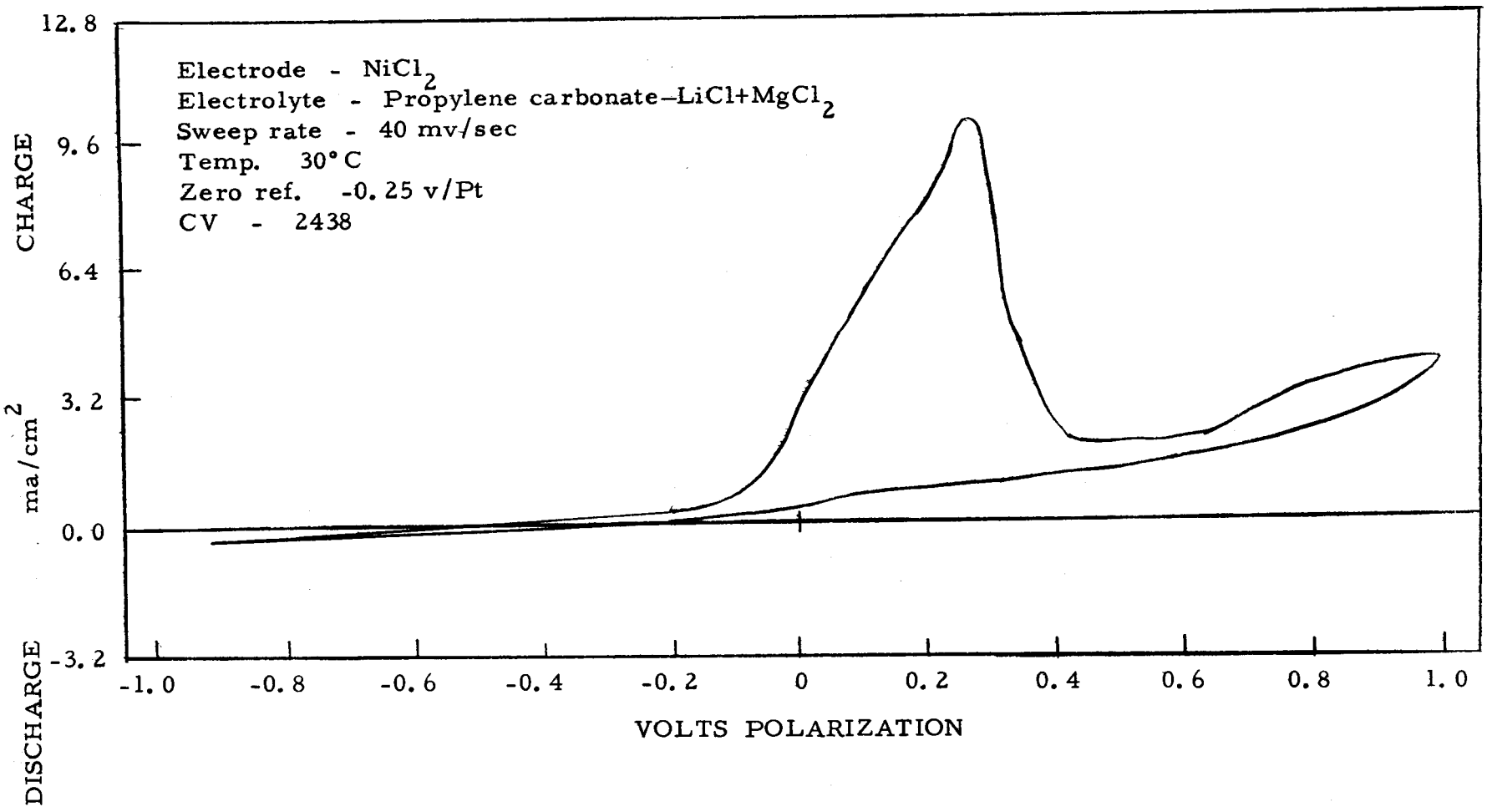
Electrode - $NiCl_2$
Electrolyte - Propylene carbonate–$LiCl+MgCl_2$
Sweep rate - 40 mv/sec
Temp. 30° C
Zero ref. -0.25 v/Pt
CV - 2438
12.8
9.6
6.4
3.2
0.0
-3.2
CHARGE
DISCHARGE
ma/cm^2
-1.0
-0.8
-0.6
-0.4
-0.2
0
0.2
0.4
0.6
0.8
1.0
VOLTS POLARIZATION

Figure 23

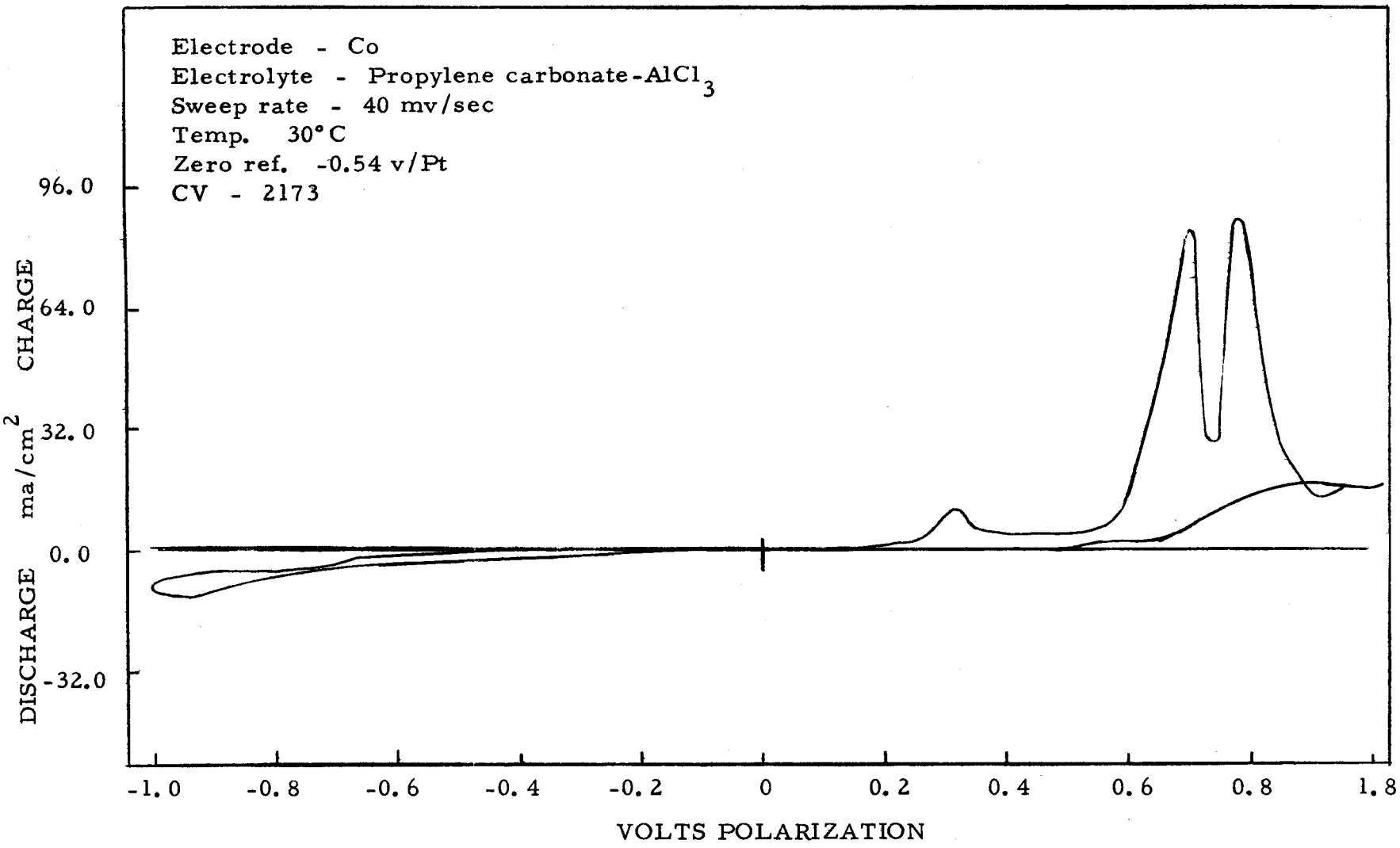
Electrode - Co
Electrolyte - Propylene carbonate-AlCl3
Sweep rate - 40 mv/sec
Temp. 30°C
Zero ref. -0.54 v/Pt
CV - 2173
96.0
64.0
32.0
0.0
-32.0
CHARGE
DISCHARGE
ma/cm2
-1.0
-0.8
-0.6
-0.4
-0.2
0
0.2
0.4
0.6
0.8
1.8
VOLTS POLARIZATION

Figure 24

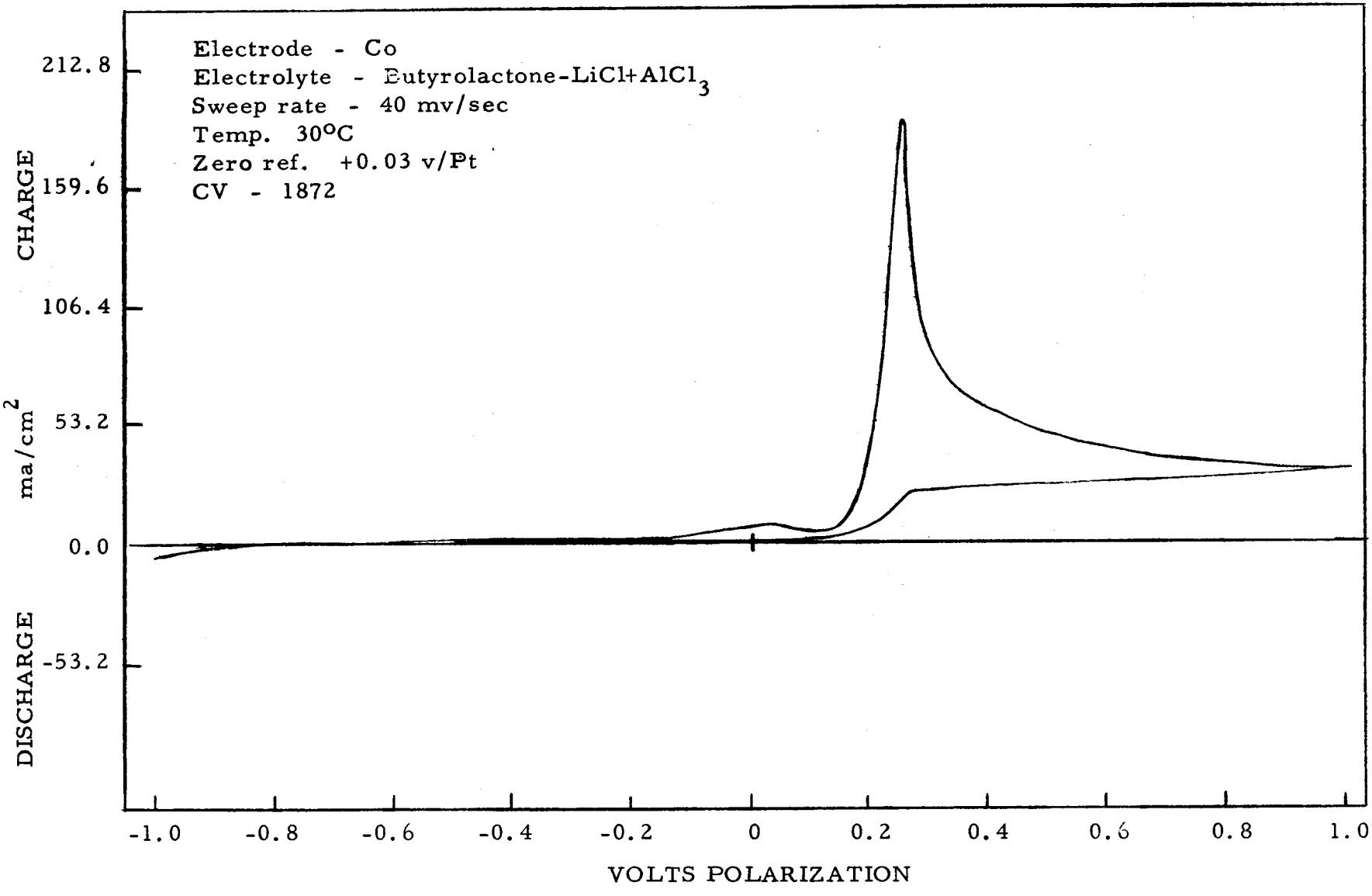
Electrode - Co
Electrolyte - Butyrolactone-LiCl+AlCl3
Sweep rate - 40 mv/sec
Temp. 30°C
Zero ref. +0.03 v/Pt
CV - 1872
212.8
159.6
106.4
53.2
0.0
-53.2
CHARGE
DISCHARGE
ma/cm2
-1.0
-0.8
-0.6
-0.4
-0.2
0
0.2
0.4
0.6
0.8
1.0
VOLTS POLARIZATION

Figure 25

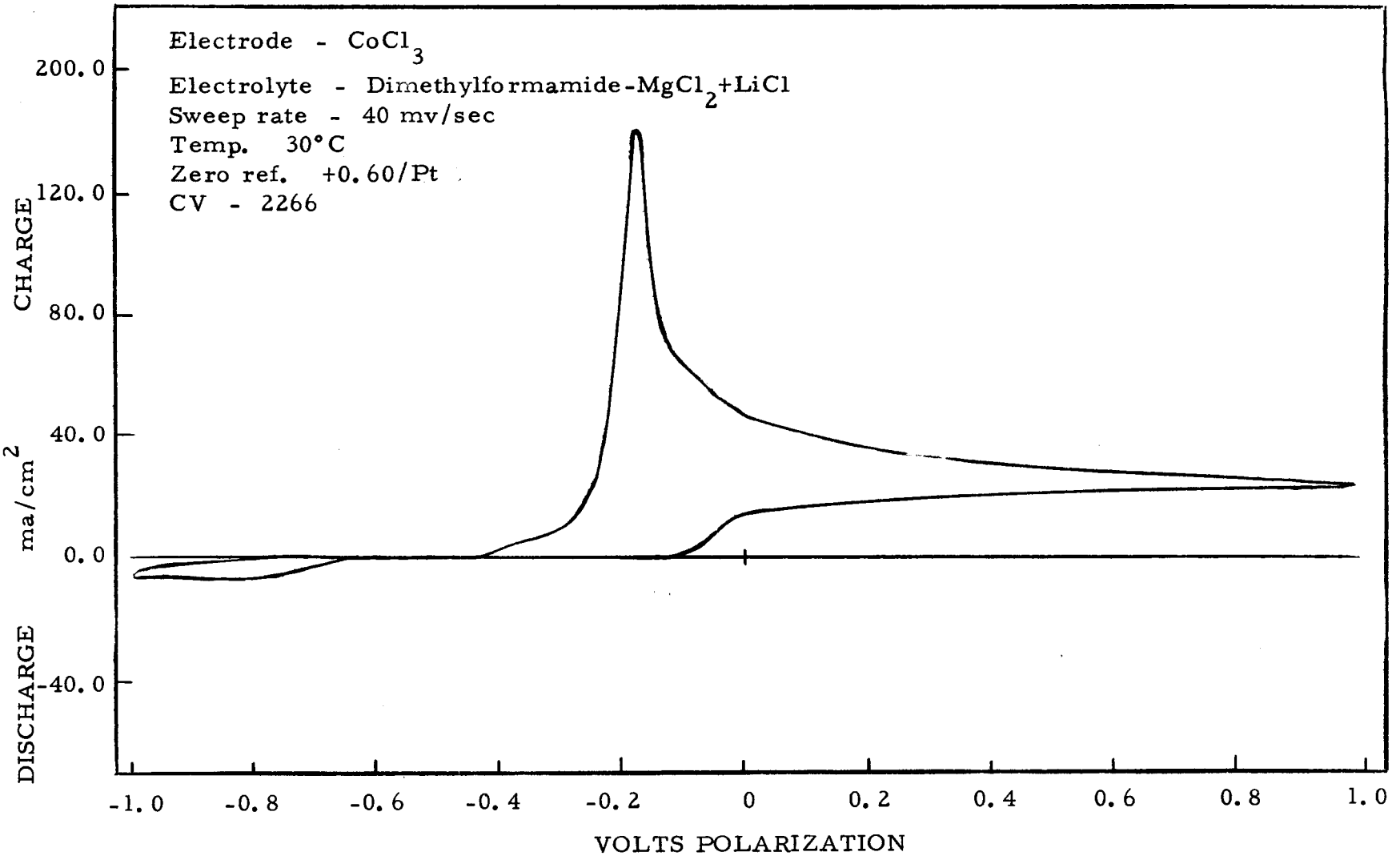
Electrode - $CoCl_3$
Electrolyte - Dimethylformamide-$MgCl_2$+LiCl
Sweep rate - 40 mv/sec
Temp. 30°C
Zero ref. +0.60/Pt
CV - 2266
200.0
120.0
80.0
40.0
0.0
-40.0
CHARGE
DISCHARGE
ma/cm^2
-1.0
-0.8
-0.6
-0.4
-0.2
0
0.2
0.4
0.6
0.8
1.0
VOLTS POLARIZATION

Figure 26

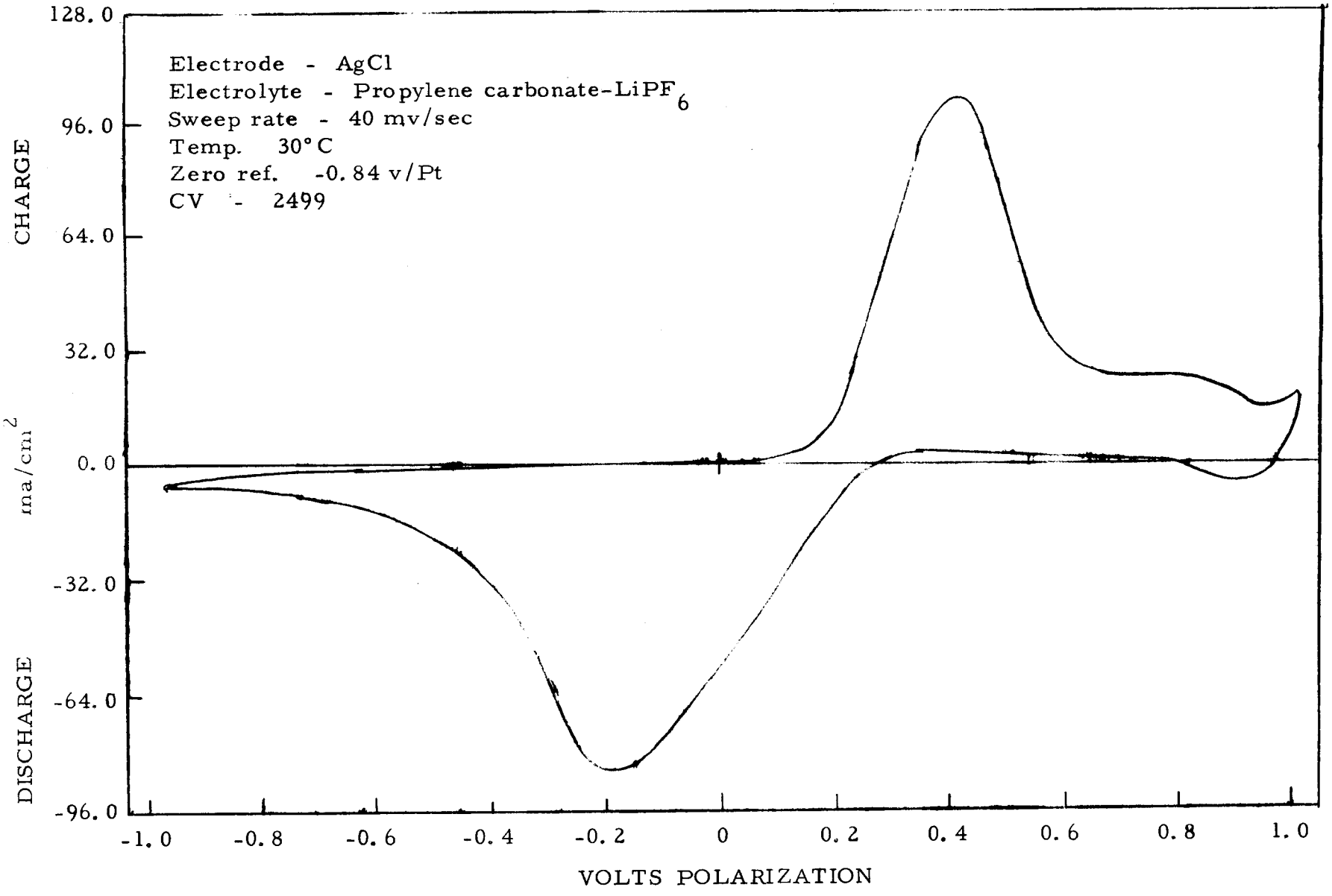
Electrode - AgCl
Electrolyte - Propylene carbonate-LiPF6
Sweep rate - 40 mv/sec
Temp. 30°C
Zero ref. -0.84 v/Pt
CV - 2499
CHARGE
DISCHARGE
ma/cm2
128.0
96.0
64.0
32.0
0.0
-32.0
-64.0
-96.0
-1.0
-0.8
-0.6
-0.4
-0.2
0
0.2
0.4
0.6
0.8
1.0
VOLTS POLARIZATION

Figure 27

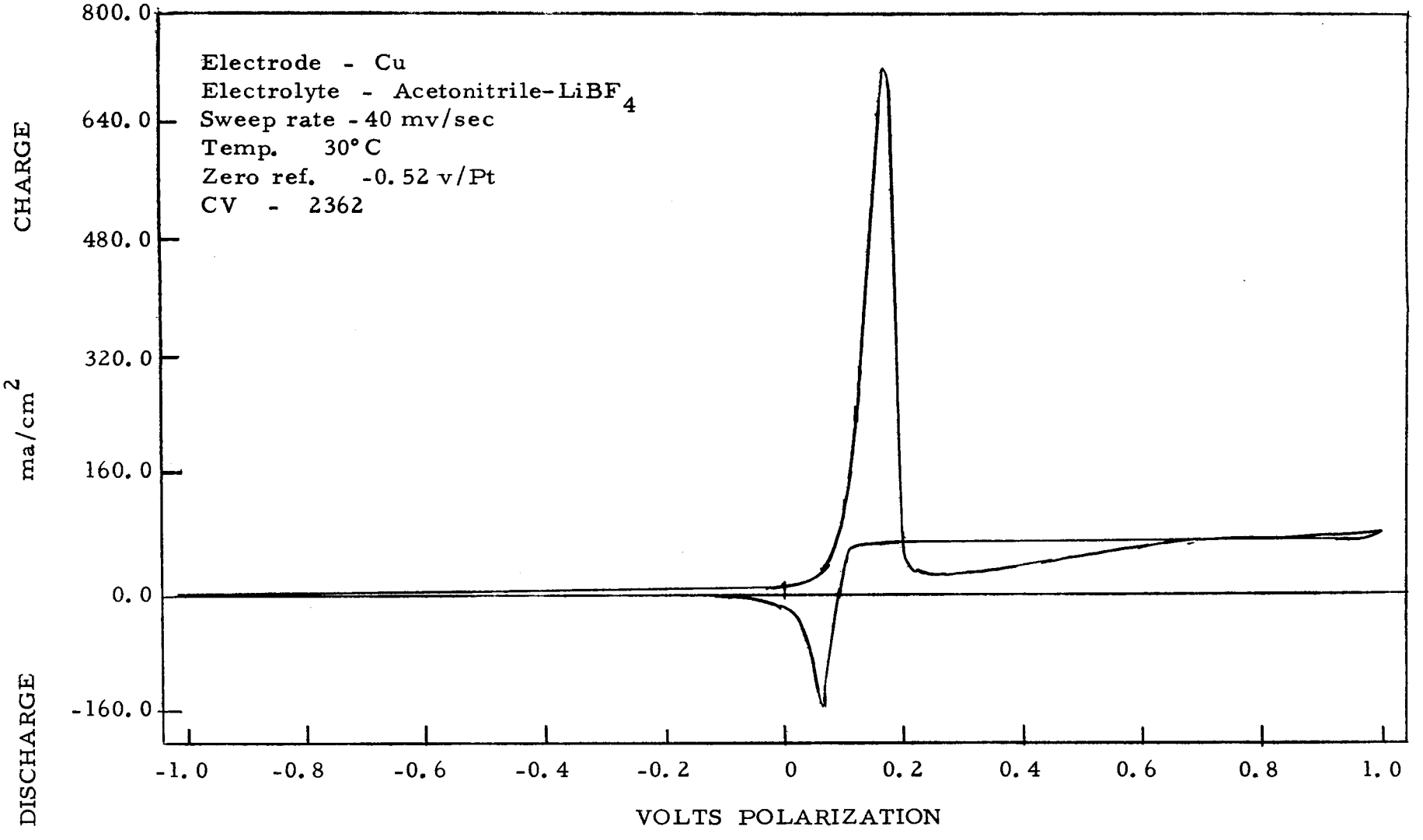
Electrode - Cu
Electrolyte - Acetonitrile-LiBF4
Sweep rate - 40 mv/sec
Temp. 30° C
Zero ref. -0.52 v/Pt
CV - 2362
800.0
640.0
480.0
320.0
160.0
0.0
-160.0
CHARGE
DISCHARGE
ma/cm2
-1.0
-0.8
-0.6
-0.4
-0.2
0
0.2
0.4
0.6
0.8
1.0
VOLTS POLARIZATION

Figure 28

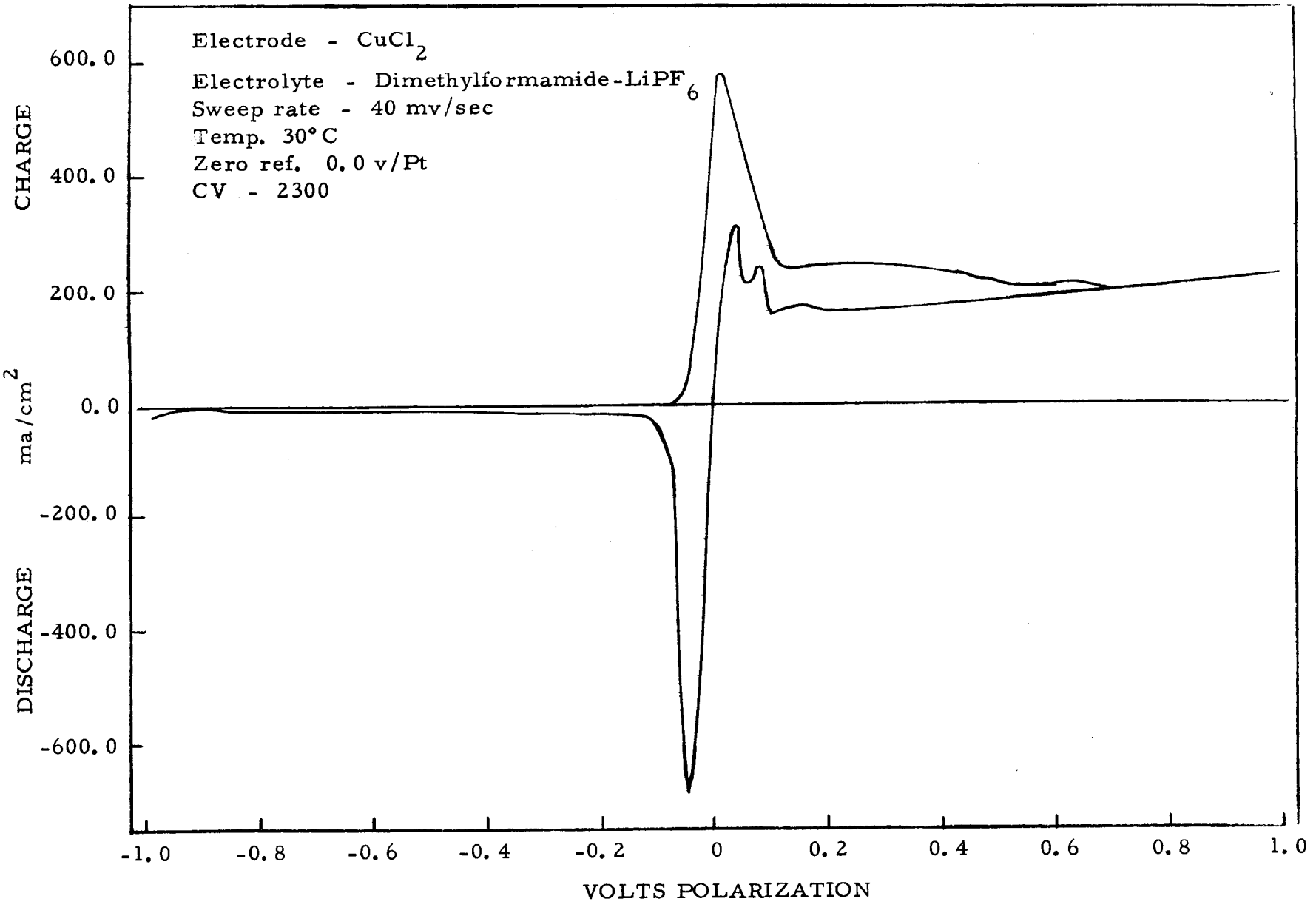
Electrode - $CuCl_2$
Electrolyte - Dimethylformamide-$LiPF_6$
Sweep rate - 40 mv/sec
Temp. 30° C
Zero ref. 0.0 v/Pt
CV - 2300
CHARGE
DISCHARGE
ma/cm^2
600.0
400.0
200.0
0.0
-200.0
-400.0
-600.0
-1.0
-0.8
-0.6
-0.4
-0.2
0
0.2
0.4
0.6
0.8
1.0
VOLTS POLARIZATION

Figure 29

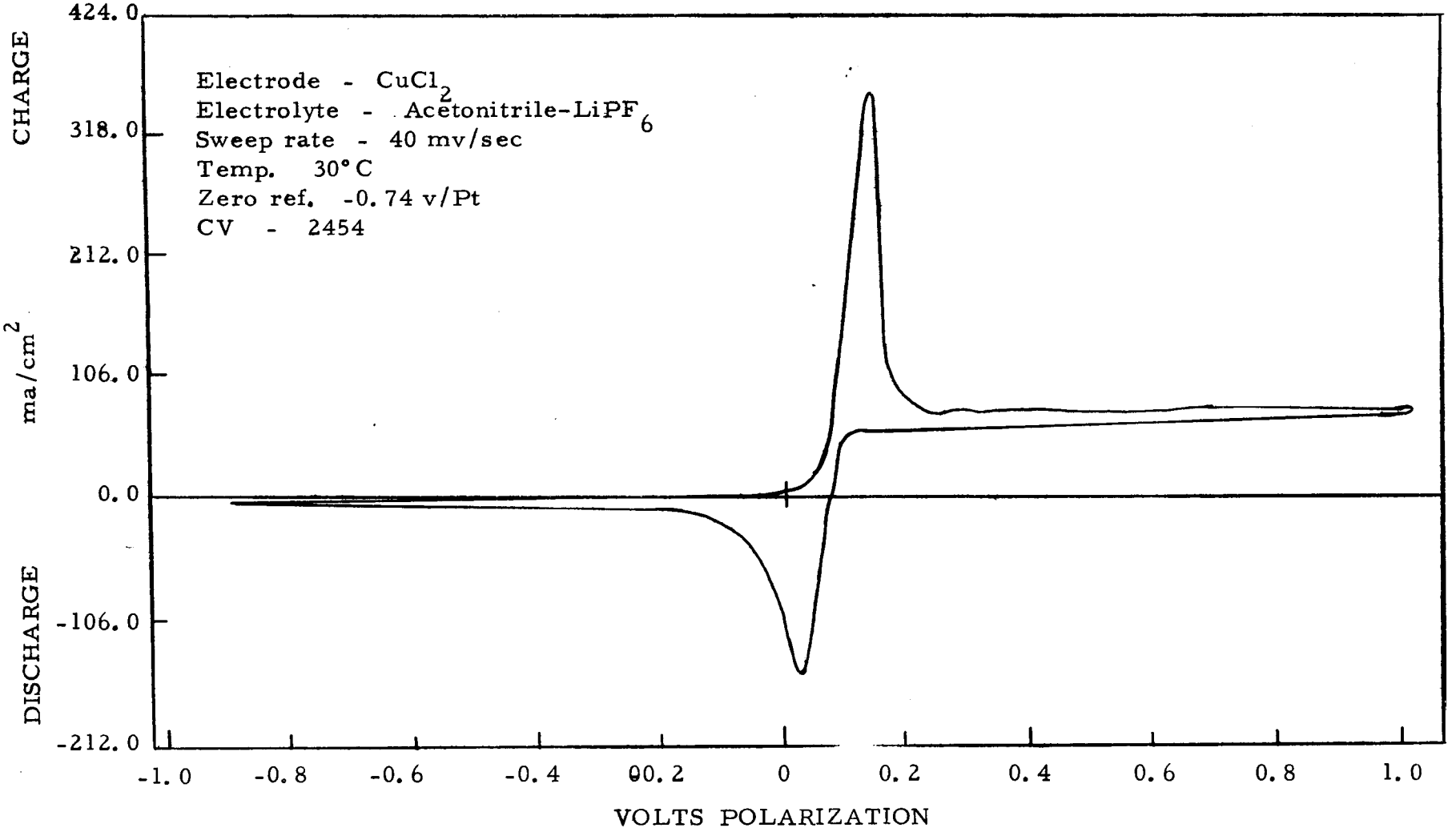
Electrode - $CuCl_2$
Electrolyte - Acetonitrile-$LiPF_6$
Sweep rate - 40 mv/sec
Temp. 30° C
Zero ref. -0.74 v/Pt
CV - 2454
CHARGE
DISCHARGE
ma/cm^2
424.0
318.0
212.0
106.0
0.0
-106.0
-212.0
-1.0
-0.8
-0.6
-0.4
-0.2
0
0.2
0.4
0.6
0.8
1.0
VOLTS POLARIZATION

Figure 30

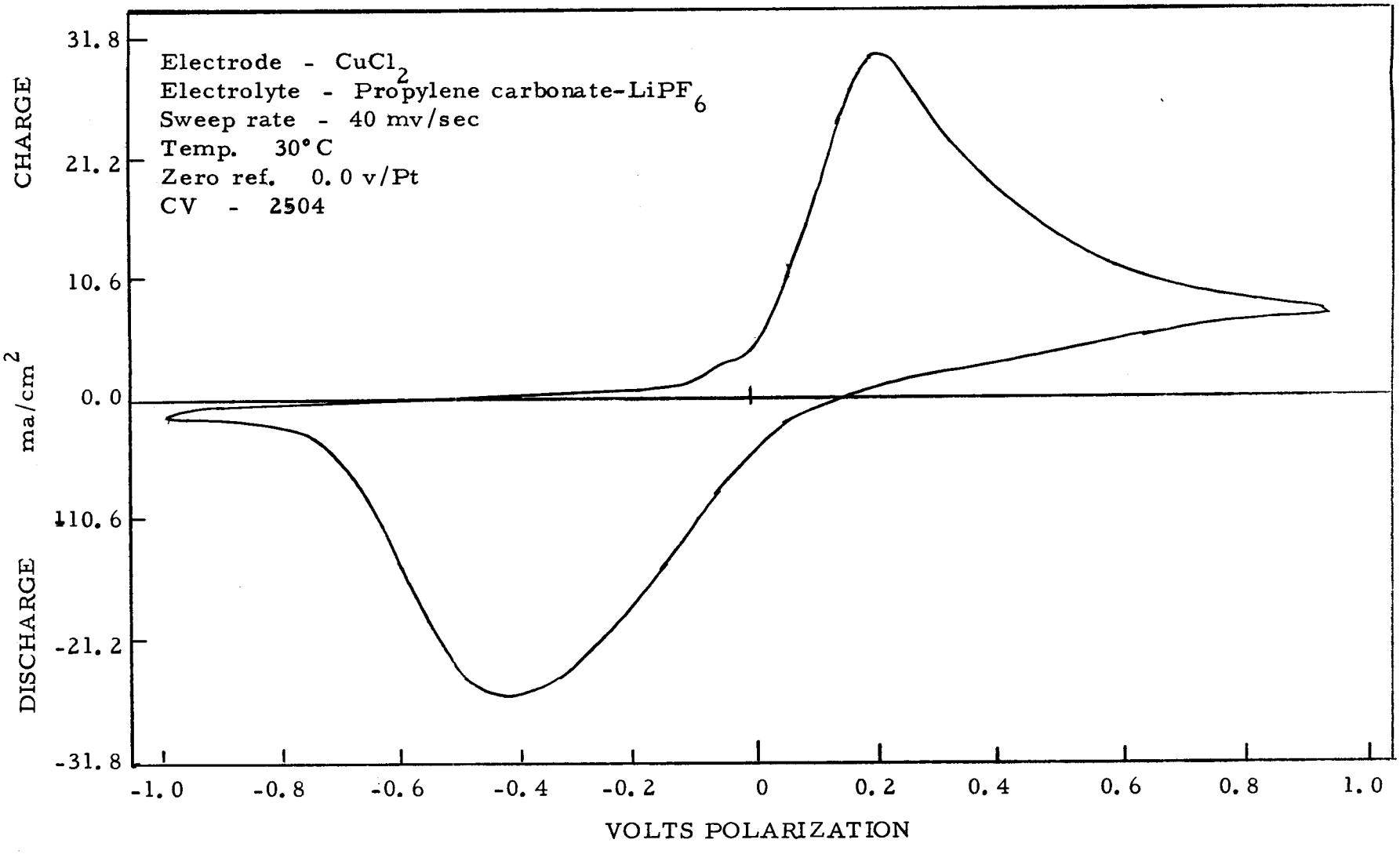
Electrode - $CuCl_2$
Electrolyte - Propylene carbonate-$LiPF_6$
Sweep rate - 40 mv/sec
Temp. 30°C
Zero ref. 0.0 v/Pt
CV - 2504
CHARGE
DISCHARGE
ma/cm^2
31.8
21.2
10.6
0.0
-10.6
-21.2
-31.8
-1.0
-0.8
-0.6
-0.4
-0.2
0
0.2
0.4
0.6
0.8
1.0
VOLTS POLARIZATION

Figure 31

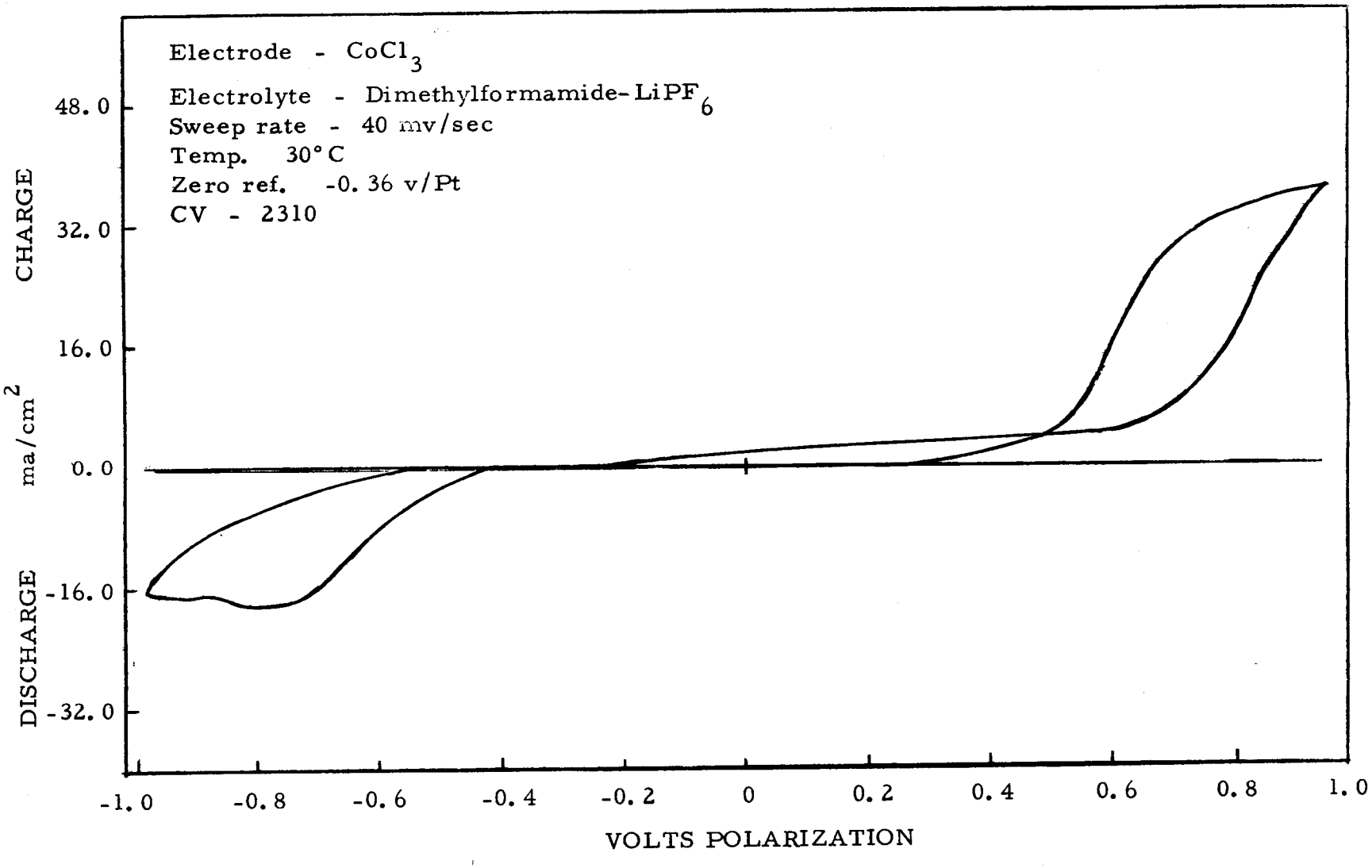
Electrode - $CoCl_3$
Electrolyte - Dimethylformamide-$LiPF_6$
Sweep rate - 40 mv/sec
Temp. 30°C
Zero ref. -0.36 v/Pt
CV - 2310
CHARGE
DISCHARGE
ma/cm^2
48.0
32.0
16.0
0.0
-16.0
-32.0
-1.0
-0.8
-0.6
-0.4
-0.2
0
0.2
0.4
0.6
0.8
1.0
VOLTS POLARIZATION

Figure 32

B. TABLES OF CYCLIC VOLTAMMETRIC DATA

Included in this section are tables listing parameters derived from the cyclic voltammograms. These parameters are as follows:

1. Sweep index - This is a relative figure of merit taking into account peak height, sweep rate, and discharge capacity. This parameter is described in more detail in an earlier report (Ref. 3, p. 80).

2. Peak current density range - Relative magnitude of peak currents classified according to page 2.

3. ΔV_p - Peak-to-peak displacement in volts of charge and discharge reactions giving a measure of overall electrode reversibility, or in more practical terms, a measure of suitability of the electrochemical system for secondary battery application.

4. Coulombic ratio - Ratio of cathodic to anodic peak area. Values significantly in excess of unity for the pre-formed electrodes (chlorinated and fluorinated metals) are indicative of the contribution of the original cathodic material to the discharge reaction independent of the material formed by the preceding charge sweep.

5. Discharge capacity - Measure of discharge utilization per unit area of electrode surface, when compared with the coulombic ratio except for values of the latter greater than unity.

Also included are tables listing the systems causing voltage and current overload of the instrumentation preventing recordable voltammograms as well as those systems failing to exhibit either anodic or cathodic peaks. No cases were found where a cathodic peak was exhibited in the absence of an anodic peak.

TABLE IV

SYSTEMS CAUSING VOLTAGE OVERLOAD
OF INSTRUMENTATION
CHLORIDE ELECTROLYTES

System	CV	Maximum Anodic Current Density ma/cm^2	Maximum Cathodic Current Density ma/cm^2
$AgCl/AN-AlCl_3$	2192	nil	1600
$AgCl/BL-MgCl_2$	2097	40	200
$AgCl/DMF-AlCl_3$	2137	1600	2000
$Cu/PC-AlCl_3+LiCl$	1851	60	2400
$CuCl_2/AN-MgCl_2$	2221	400	nil
$NiO/DMF-AlCl_3$	2141	2400	nil
$NiCl_2/DMF-LiCl+MgCl_2$	2287	1470	nr *
$Co/AN-MgCl_2$	2211	80	nil
$Co/BL-MgCl_2$	2095	400	nil
$Co/DMF-AlCl_3$	2139	2400	nil
$CoO/AN-MgCl_2$	2210	180	nil
$CoO/BL-MgCl_2$	2094	400	nil
$CoO/DMF-AlCl_3$	2138	2400	nil
$CoCl_3/AN-MgCl_2$	2212	80	nil
$CoCl_3/BL-MgCl_2$	2096	400	nil
$CoCl_3/DMF-AlCl_3$	2140	2400	nil

AN - Acetonitrile
BL - Butyrolactone
DMF - Dimethylformamide
PC - Propylene carbonate

* - not recorded

TABLE V

SYSTEMS CAUSING VOLTAGE OVERLOAD
OF INSTRUMENTATION
FLUORIDE ELECTROLYTES

System	CV	Maximum Anodic Current Density ma/cm^2	Maximum Cathodic Current Density ma/cm^2
Ag/PC-$LiBF_4$	2383	3200	400
Ag/PC-$Mg(BF_4)_2$	2400	200	200
AgF_2/AN-$Mg(BF_4)_2$	2414	1600	nil
AgF_2/AN-BF_3	2329	200	200
AgF_2/AN-PF_5	2465	2000	2000
AgF_2/BL-BF_3	2335	600	400
AgF_2/DMF-$Mg(BF_4)_2$	2390	4000	3200
AgF_2/DMF-BF_3	2311	1200	1600
AgF_2/DMF-PF_5	2475	2400	2400
AgF_2/PC-$Mg(BF_4)_2$	2404	200	200
AgF_2/PC-BF_3	2321	200	200
AgF_2/PC-PF_5	2485	600	400
Cu/PC-$LiBF_4$	2384	2160	2400
Cu/PC-$Mg(BF_4)_2$	2401	400	80
CuF_2/AN-$Mg(BF_4)_2$	2415	1600	600
CuF_2/AN-BF_3	2330	600	200
CuF_2/AN-PF_5	2466	1600	1200
CuF_2/BL-BF_3	2336	400	40

AN - Acetonitrile
BL - Butyrolactone
DMF - Dimethylformamide
PC - Propylene carbonate

TABLE V (Cont'd.)

System	CV	Maximum Anodic Current Density ma/cm^2	Maximum Cathodic Current Density ma/cm^2
CuF_2/DMF-$Mg(BF_4)_2$	2391	4000	1600
CuF_2/DMF-BF_3	2312	1600	nil
CuF_2/DMF-PF_5	2476	1600	1600
CuF_2/PC-$Mg(BF_4)_2$	2405	200	40
CuF_2/PC-BF_3	2322	2000	nil
CuF_2/PC-PF_5	2486	400	400
Ni/PC-$Mg(BF_4)_2$	2402	40	nil
NiF_2/AN-BF_3	2331	200	nil
NiF_2/BL-BF_3	2337	200	nil
Co/PC-$Mg(BF_4)_2$	2403	40	40

AN - Acetonitrile
BL - Butyrolactone
DMF - Dimethylformamide
PC - Propylene carbonate

TABLE VI

SYSTEMS CAUSING CURRENT OVERLOAD*
OF INSTRUMENTATION

System	CV	Maximum Anodic Current Density ma/cm^2	Maximum Cathodic Current Density ma/cm^2
$Ag/AN-LiBF_4$	2357	ov*	nil
$Ag/DMF-LiBF_4$	2369	ov	nr**
$AgCl/AN-LiClO_4$	2005	ov	ov
AgCl/BL-LiCl	2050	ov	ov
$AgCl/BL-LiClO_4$	2022	ov	ov
$AgCl/BL-LiCl+LiClO_4$	2341	ov	ov
$AgCl/DMF-LiClO_4$	1970	ov	ov
$AgCl/DMF-LiPF_6$	2298	400	ov
$AgCl/PC-LiClO_4$	1989	ov	nr
$CuCl_2/AN-AlCl_3$	2191	ov	ov
$CuCl_2/PC-AlCl_3+LiCl$	1832	2000	ov
$NiCl_2/AN-AlCl_3$	2189	ov	nil
$NiCl_2/AN-AlCl_3+LiCl$	1960	ov	20
$NiCl_2/DMF-AlCl_3+LiCl$	1903	ov	nil
$NiF_2/AN-AlCl_3+LiCl$	1942	ov	nil
$Co/AN-AlCl_3+LiCl$	1958	ov	nil
$CoO/AN-AlCl_3+LiCl$	1959	ov	12
$CoCl_3/AN-AlCl_3+LiCl$	1961	ov	nil
$CoCl_3/DMF-AlCl_3+LiCl$	1909	ov	nil

* ov - maximum current greater than 4.8 amp/cm^2
** nr - not recorded

AN - Acetonitrile
BL - Butyrolactone
DMF - Dimethylformamide
PC - Propylene carbonate

TABLE VII

PEAK CURRENT DENSITY RANGE
CHLORIDE AND PERCHLORATE ELECTROLYTES

System	CV	Anodic	Cathodic
$AgCl/AN-AlCl_3+LiCl$	1969	very high	very high
$AgCl/AN-MgCl_2$	2226	low	low
$AgCl/BL-AlCl_3$	2209	very high	very high
$AgCl/BL-AlCl_3+LiCl$	1887	high	high
$AgCl/BL-LiCl+MgCl_2$	2251	medium low	medium high
$AgCl/DMF-LiCl$	2038	very high	very high
$AgCl/DMF-AlCl_3+LiCl$	1914	high	very high
$AgCl/DMF-LiCl+LiClO_4$	2231	medium high	high
$AgCl/DMF-MgCl_2$	2131	high	high
$AgCl/DMF-LiCl+MgCl_2$	2281	medium low	high
$AgCl/PC-AlCl_3$	2148	very high	very high
$AgCl/PC-MgCl_2$	2069	medium low	medium low
$AgCl/PC-LiCl+MgCl_2$	2428	low	low
$AgF_2/AN-AlCl_3+LiCl$	1952	low	medium low
$AgF_2/DMF-AlCl_3+LiCl$	1831	very low	very low
$AgF_2/PC-AlCl_3+LiCl$	1842	very low	low
$CuCl_2/AN-LiClO_4$	2020	high	medium high
$CuCl_2/BL-LiCl$	2049	high	medium high
$CuCl_2/BL-AlCl_3$	2208	very high	very high
$CuCl_2/BL-AlCl_3+LiCl$	1902	very high	high
$CuCl_2/BL-LiClO_4$	2021	very high	very high
$CuCl_2/BL-LiCl+LiClO_4$	2346	high	very high
$CuCl_2/BL-MgCl_2$	2105	medium high	medium high
$CuCl_2/BL-LiCl+MgCl_2$	2256	high	medium low

AN - Acetonitrile
BL - Butyrolactone
DMF - Dimethylformamide
PC - Propylene carbonate

TABLE VII (Cont'd.)

System	CV	Anodic	Cathodic
$CuCl_2$/AN-$AlCl_3$+LiCl	1962	very high	very high
$CuCl_2$/DMF-$AlCl_3$	2146	very high	very high
$CuCl_2$/DMF-$AlCl_3$+LiCl	1988	very high	very high
$CuCl_2$/DMF-LiCl+$LiClO_4$	2236	high	high
$CuCl_2$/DMF-$MgCl_2$	2136	medium low	medium low
$CuCl_2$/DMF-LiCl+$MgCl_2$	2286	high	very high
$CuCl_2$/PC-$AlCl_3$	2147	high	very high
$CuCl_2$/PC-$AlCl_3$+LiCl	1928	very high	very high
$CuCl_2$/PC-$LiClO_4$	1999	very high	very high
$CuCl_2$/PC-$MgCl_2$	2064	medium low	medium low
$CuCl_2$/PC-LiCl+$MgCl_2$	2433	medium low	low
CuF_2/AN-$AlCl_3$+LiCl	1957	high	medium high
CuF_2/BL-$AlCl_3$+LiCl	1877	low	low
CuF_2/BL-$AlCl_3$+LiCl	1882	very high	high
CuF_2/DMF-$AlCl_3$+LiCl	1817	very high	very high
CuF_2/PC-$AlCl_3$+LiCl	1837	high	very high
$NiCl_2$/BL-LiCl	2056	medium high	medium low
$NiCl_2$/DMF-LiCl+$LiClO_4$	2241	very high	medium low
$NiCl_2$/PC-$AlCl_3$+LiCl	1934	low	very low
Co/PC-$AlCl_3$	2173	medium high	medium low
CoO/PC-$AlCl_3$	2168	medium low	low
$CoCl_3$/BL-LiCl	2051	very high	medium low
$CoCl_3$/BL-$AlCl_3$+LiCl	1892	high	low
$CoCl_3$/BL-$LiClO_4$	2027	medium low	medium low
$CoCl_3$/BL-LiCl+$MgCl_2$	2266	high	low
$CoCl_3$/PC-$AlCl_3$	2163	medium high	medium low

AN - Acetonitrile
BL - Butyrolactone
DMF - Dimethylformamide
PC - Propylene carbonate

TABLE VIII

PEAK CURRENT DENSITY RANGE
FLUORIDE ELECTROLYTES

System	CV	Anodic	Cathodic
$AgCl/AN-LiPF_6$	2449	very high	high
$AgCl/PC-LiPF_6$	2499	high	medium high
$AgF_2/BL-LiF+KPF_6$	1807	low	low
$Cu/AN-LiBF_4$	2362	very high	high
$CuCl_2/AN-LiPF_6$	2454	very high	high
$CuCl_2/DMF-LiPF_6$	2300	very high	very high
$CuCl_2/PC-LiPF_6$	2504	medium low	medium low
$CuF_2/BL-LiF+KPF_6$	1812	high	medium low
$Ni/PC-LiBF_4$	2389	low	low
$CoCl_3/AN-LiPF_6$	2464	medium high	medium high
$CoCl_3/DMF-LiPF_6$	2310	medium low	medium low
$CoCl_3/PC-LiPF_6$	2514	low	low

AN - Acetonitrile
BL - Butyrolactone
DMF - Dimethylformamide
PC - Propylene carbonate

TABLE IX

SWEEP INDEX*

System	CV	Anodic $ohm^{-1} cm^{-2}$	Cathodic $ohm^{-1} cm^{-2}$
$AgCl/AN-LiCl+AlCl_3$	1969	530.0	514.3
$AgCl/BL-AlCl_3$	2209	496.0	605.0
$AgCl/BL-LiCl+AlCl_3$	1887	17.5	27.8
$AgCl/BL-LiCl+MgCl_2$	2251	4.6	11.1
$AgCl/DMF-LiCl+AlCl_3$	1914	42.6	250.0
$AgCl/DMF-LiCl+MgCl_2$	2281	-	112.0
$AgCl/PC-MgCl_2$	2069	9.9	4.8
$AgCl/PC-LiCl+MgCl_2$	2428	0.1	0.6
$AgCl/PC-LiPF_6$	2499	26.5	17.6
$AgF_2/AN-LiCl+AlCl_3$	1952	0.6	1.6
$Cu/AN-LiBF_4$	2362	1120.0	248.0
$CuCl_2/AN-LiPF_6$	2454	368.0	141.0
$CuCl_2/BL-AlCl_3$	2208	548.0	1330.0
$CuCl_2/BL-MgCl_2$	2105	91.1	80.8
$CuCl_2/BL-LiClO_4$	2021	357.0	712.0
$CuCl_2/DMF-MgCl_2$	2136	-	34.0
$CuCl_2/DMF-LiCl+MgCl_2$	2286	-	2405.0
$CuCl_2/DMF-LiPF_6$	2300	-	1026.0
$CuCl_2/PC-AlCl_3$	2147	88.9	755.0
$CuCl_2/PC-LiClO_4$	1999	162.9	864.0
$CuCl_2/PC-LiCl+MgCl_2$	2433	1.6	1.3
$CuCl_2/PC-LiPF_6$	2504	6.0	5.1
$CuF_2/BL-LiCl+AlCl_3$	1882	487.0	33.2
$CuF_2/PC-LiCl+AlCl_3$	1837	-	276.0

AN - Acetonitrile
BL - Butyrolactone
DMF - Dimethylformamide
PC - Propylene carbonate

$$*\frac{(\text{peak c. d.})^2 \times 100}{\text{sweep rate} \times \text{coul/cm}^2}$$

TABLE X

ΔV_p, COULOMBIC RATIO,° AND DISCHARGE CAPACITY

System	CV	ΔV_p*	Coulombic ** Ratio	Discharge Capacity coul/cm^2
$AgCl/AN-LiCl+AlCl_3$	1969	0.49	1.17	3.11
$AgCl/BL-AlCl_3$	2209	0.55	3.50	3.87
$AgCl/BL-LiCl+AlCl_3$	1887	----	0.98	2.65
$AgCl/BL-LiCl+MgCl_2$	2251	0.75	0.98	0.74
$AgCl/DMF-LiCl$	2038	0.08	----	----
$AgCl/DMF-LiCl+AlCl_3$	1914	----	0.56	1.15
$AgCl/DMF-LiCl+MgCl_2$	2281	0.29	0.83	0.58
$AgCl/PC-MgCl_2$	2069	0.58	0.93	0.27
$AgCl/PC-LiCl+MgCl_2$	2428	0.5	1.23	0.04
$AgCl/PC-LiPF_6$	2499	0.62	1.00	1.10
$AgF_2/AN-LiCl+AlCl_3$	1952	0.65	1.96	0.23
$Cu/AN-LiBF_4$	2362	0.10	0.23	0.23
$CuCl_2/AN-LiPF_6$	2454	0.11	0.50	0.43
$CuCl_2/BL-AlCl_3$	2208	0.30	0.99	4.83
$CuCl_2/BL-LiClO_4$	2021	0.19	0.71	0.25
$CuCl_2/Bl-MgCl_2$	2105	----	1.04	0.18
$CuCl_2/DMF-LiCl+LiClO_4$	2236	0.24	0.25	0.66
$CuCl_2/DMF-LiPF_6$	2300	0.06	0.98	0.11
$CuCl_2/PC-AlCl_3$	2147	0.47	1.65	4.28
$CuCl_2/PC-LiClO_4$	1999	0.16	1.03	2.94

* - Voltage separating anodic to cathodic peaks

** - Ratio of cathodic to anodic peak areas

AN - Acetonitrile
BL - Butyrolactone
DMF - Dimethylformamide
PC - Propylene carbonate

TABLE X (Cont'd.)

System	CV	ΔV_p*	Coulombic** Ratio	Discharge Capacity coul/cm^2
$CuCl_2$/PC-LiCl+$MgCl_2$	2433	0.63	1.00	0.22
$CuCl_2$/PC-$LiPF_6$	2504	0.60	0.86	0.33
$CoCl_3$/AN-$LiClO_4$	2010	1.45	----	----
$CoCl_3$/AN-$LiPF_6$	2464	1.27	----	----
$CoCl_3$/BL-$LiClO_4$	2027	1.40	----	----
$NiCl_2$/BL-LiCl	2056	1.00	----	----

* - Voltage separating anodic to cathodic peaks

** - Ratio of cathodic to anodic peak areas

AN - Acetonitrile
BL - Butyrolactone
DMF - Dimethylformamide
PC - Propylene carbonate

TABLE XI

SYSTEMS EXHIBITING ANODIC PEAK ONLY
CHLORIDE AND PERCHLORATE ELECTROLYTES*

System	CV		Peak Current Density Range
$NiO/PC-AlCl_3$	2158		medium low
$NiCl_2/AN-MgCl_2$	2220		very low
$NiCl_2/BL-AlCl_3$	2207		low
$NiCl_2/BL-AlCl_3+LiCl$	1897		low
$NiCl_2/BL-LiClO_4$	2032		low
$NiCl_2/BL-LiCl+LiClO_4$	2356	a	low
$NiCl_2/PC-MgCl_2$	2093		very low
$NiCl_2/PC-LiCl+MgCl_2$	2438		low
$NiF_2/BL-AlCl_3+LiCl$	1859		medium low
$NiF_2/DMF-AlCl_3+LiCl$	1828		low
$NiF_2/PC-AlCl_3+LiCl$	1850		very low
$Co/AN-AlCl_3$	2183		high
$Co/BL-AlCl_3$	2202	a	high
$Co/BL-AlCl_3+LiCl$	1872		high
$Co/DMF-MgCl_2$	2120		very low
$Co/PC-AlCl_3+LiCl$	1847	b	medium high
$Co/PC-MgCl_2$	2074		high
$Co/PC-LiCl+MgCl_2$	2443		high

* - Maximum cathodic current density in very low range (< 1 ma/cm^2) unless otherwise noted

a - Low range cathodic (< 10 ma/cm^2)

b - Medium low range cathodic (10-50 ma/cm^2)

AN - Acetonitrile
BL - Butyrolactone
DMF - Dimethylformamide
PC - Propylene carbonate

TABLE XI (Cont'd.) *

System	CV		Peak Current Density Range
$CoO/AN-AlCl_3$	2178		very high
$CoO/BL-AlCl_3+LiCl$	1864		low
$CoO/DMF-MgCl_2$	2115		very high
$CoCl_3/AN-AlCl_3$	2188		very high
$CoCl_3/BL-AlCl_3$	2197		high
$CoCl_3/BL-LiCl+LiClO_4$	2351	a	medium low
$CoCl_3/DMF-MgCl_2$	2125		very low
$CoCl_3/PC-AlCl_3+LiCl$	1941	b	medium high
$CoCl_3/PC-MgCl_2$	2090		medium high
$CoCl_3/PC-LiCl+MgCl_2$	2448		medium high
$CoF_3/BL-AlCl_3+LiCl$	1867		very low
$CoF_3/DMF-AlCl_3+LiCl$	1822		very low
$CoF_3/PC-AlCl_3+LiCl$	1854		very low

* - Maximum cathodic current density in very low range (< 1 ma/cm^2) unless otherwise noted

a - Low range cathodic (< 10 ma/cm^2)

b - Medium low range cathodic (10-50 ma/cm^2)

AN - Acetonitrile
BL - Butyrolactone
DMF - Dimethylformamide
PC - Propylene carbonate

TABLE XII

SYSTEMS EXHIBITING ANODIC PEAK ONLY
FLUORIDE ELECTROLYTES*

System	CV	Peak Current Density Range
$Cu/DMF-LiBF_4$	2372	very high
$Ni/AN-LiBF_4$	2367	very high
$Ni/DMF-LiBF_4$	2377	low
$NiCl_2/AN-LiPF_6$	2459	medium low
$NiCl_2/PC-LiPF_6$	2509	low
$NiF_2/AN-Mg(BF_4)_2$	2420	high
$NiF_2/AN-PF_5$	2471	very low
$NiF_2/DMF-Mg(BF_4)_2$	2396	low
$NiF_2/DMF-BF_3$	2317	medium low
$NiF_2/DMF-PF_5$	2481	low
$NiF_2/PC-Mg(BF_4)_2$	2410	low
$Co/AN-LiBF_4$	2368	very high
$Co/DMF-LiBF_4$	2382	very high

* - Maximum cathodic current density in very low range (<1 ma/cm^2)

AN - Acetonitrile
BL - Butyrolactone
DMF - Dimethylformamide
PC - Propylene carbonate

TABLE XIII

SYSTEMS EXHIBITING NO PEAKS
CHLORIDE AND PERCHLORATE ELECTROLYTES*

System	CV	
$AgCl/PC-AlCl_3+LiCl$	1933	a
$CuCl_2/DMF-LiCl$	2037	
$CuCl_2/DMF-LiClO_4$	1978	
$NiO/PC-MgCl_2$	2075	
$NiCl_2/AN-LiClO_4$	2015	ab
$NiCl_2/BL-MgCl_2$	2098	
$NiCl_2/BL-LiCl+MgCl_2$	2261	
$NiCl_2/DMF-LiCl$	2048	
$NiCl_2/DMF-LiClO_4$	1971	
$NiCl_2/DMF-MgCl_2$	2130	
$NiCl_2/PC-AlCl_3$	2153	
$NiCl_2/PC-LiClO_4$	1994	a
$Co/DMF-LiCl+MgCl_2$	2297	
$CoO/BL-LiCl+MgCl_2$	2276	
$CoO/DMF-AlCl_3+LiCl$	1908	c
$CoO/PC-AlCl_3+LiCl$	2059	
$CoO/PC-MgCl_2$	2082	
$CoCl_3/DMF-LiCl$	2043	
$CoCl_3/DMF-LiClO_4$	1983	ab

* - Maximum current density in very low range (<1 ma/cm^2) unless otherwise noted

a - Low range anodic (<10 ma/cm^2)

b - Low range cathodic (<10 ma/cm^2)

c - Medium low range anodic (10-50 ma/cm^2)

AN - Acetonitrile
BL - Butyrolactone
DMF - Dimethylformamide
PC - Propylene carbonate

TABLE XIII (Cont'd.) *

System	CV	
$CoCl_3$/DMF-LiCl+$LiClO_4$	2246	b
$CoCl_3$/DMF-LiCl+$MgCl_2$	2292	
$CoCl_3$/PC-$LiClO_4$	2004	
CoF_3/AN-$AlCl_3$+LiCl	1947	
CoF_3/AN-$MgCl_2$	2215	
CoF_3/ DMF-$MgCl_2$	2110	
CoF_3/PC-$MgCl_2$	2085	

* - Maximum current density in very low range (<1 ma/cm^2) unless otherwise noted

b - Low range cathodic (<10 ma/cm^2)

AN - Acetonitrile
BL - Butyrolactone
DMF - Dimethylformamide
PC - Propylene carbonate

TABLE XIV

SYSTEMS EXHIBITING NO PEAKS
FLUORIDE ELECTROLYTES*

System	CV	
AgF_2/AN-BF_3	2328	
$NiCl_2$/DMF-$LiPF_6$	2305	a
NiF_2/PC-PF_5	2491	
CoF_3/AN-$Mg(BF_4)_2$	2421	
CoF_3/AN-BF_3	2334	
CoF_3/AN-PF_5	2474	
CoF_3/BL-LiCl+$MgCl_2$	2271	
CoF_3/BL-LiF+KPF_6	1802	a
CoF_3/BL-BF_3	2340	
CoF_3/DMF-$Mg(BF_4)_2$	2399	
CoF_3/DMF-BF_3	2320	
CoF_3/DMF-PF_5	2484	
CoF_3/PC-$Mg(BF_4)_2$	2411	
CoF_3/PC-PF_5	2494	
NiF_2/PC-BF_3	2325	

* - Maximum current density in very low range (< 1 ma/cm^2) unless otherwise noted

a - Medium low range (10-50 ma/cm^2)

AN - Acetonitrile
BL - Butyrolactone
DMF - Dimethylformamide
PC - Propylene carbonate

II. REFERENCES

1. Whittaker Corp., Narmco R and D Div., Second Quarterly Report, NASA contract NAS 3-8509, NASA report CR-72138, November 1966.

2. Whittaker Corp., Narmco R and D Div., Third Quarterly Report, NASA contract NAS 3-8509, NASA report CR-72181, February 1967.

3. Whittaker Corp., Narmco R and D Div., First Quarterly Report, NASA contract NAS 3-8509, NASA report CR-72069, August 1966.